
Auto-Encoding Sequential Monte Carlo

Tuan Anh Le Maximilian Igl Tom Jin Tom Rainforth Frank Wood
 {tuananh, migl, jin, twgr, fwood}@robots.ox.ac.uk
 Department of Engineering Science, Oxford

Abstract

We introduce auto-encoding sequential Monte Carlo (AESMC): a method for using deep neural networks for simultaneous model learning and inference amortization in a broad family of structured probabilistic models. Starting with an unlabeled dataset and a partially specified underlying generative model, AESMC refines the generative model and learns efficient proposal distributions for sequential Monte Carlo (SMC) for performing inference in this model. Our approach relies on 1) efficiency of SMC in performing inference in structured probabilistic models and 2) flexibility of deep neural networks to model complex conditional probability distributions. We demonstrate that our approach provides a fast, accurate, easy-to-implement, and scalable means for carrying out parameter estimation in high-dimensional statistical models as well as simultaneous model learning and proposal amortization in neural network based models.

1 Introduction

Probabilistic machine learning [Ghahramani, 2015] allows us to model the structure and dependencies of latent variables and observational data as a joint probability distribution. Once a model is defined, we can perform inference to update our prior beliefs about latent variables in light of observed data to obtain the posterior distribution. The posterior can be used to answer any questions we might have about the latent quantities while coherently accounting for our uncertainty about the world.

We introduce a method for simultaneous model learning and inference amortization [Gershman and Goodman, 2014], given an unlabeled dataset of observations. The model is specified partially, the rest being specified using a *generative network* whose weights are to be learned. Inference amortization refers to spending additional time before inference to obtain an amortization artifact which is used to speed up inference during test time. We amortize inference by learning a *proposal network* which maps from observations to parameters of proposal distributions for efficient inference using SMC [Doucet and Johansen, 2009]. We show that by maximizing the SMC based log evidence estimator with respect to both generative and proposal network parameters, we obtain simultaneous model learning and inference amortization.

Our contributions are three-fold. First, we devise a method for differentiating through the resampling step of SMC. The key insight is to consider the SMC evidence estimator to be a random variable which is a function of all random variables in the SMC algorithm, including the ancestral indices and particle values. Once these random variables are fixed, the computation graph is deterministic and only consists of differentiable SMC weight calculations. As the expectation of the marginal likelihood estimates over these variables is equal to the true marginal likelihood, each such gradient evaluation is itself an unbiased estimate of the true gradient and can thus be used in a stochastic gradient descent (SGD) algorithm. This gives a simple to implement, but highly effective approach for model learning.

Second, we introduce a proposal network and show how it is possible to perform simultaneous model learning and proposal adaptation by performing SGD on the parameters of both. We develop an evidence lower bound (ELBO) and show that this is optimized when the model evidence is optimized, the intermediary SMC targets are the corresponding marginal distributions given the full

dataset, and the corresponding optimal proposal is used. Consequently, if this ELBO optimized, all samples produced from the learnt SMC scheme correspond to *exact* samples from the model which optimizes. Though we derive how exact derivatives of this ELBO can be calculated, we also provide approximations that significantly reduce the variance of the resulting gradients at the expense of a small degree of bias. We demonstrate empirically that the resulting biased gradient scheme outperforms previous approaches.

Third, we show that this approach can be extended to an amortized inference setting, learning an artifact that takes in a dataset at run time and provides the optimal model and proposal for that dataset. Unlike previous similar approaches, e.g. [Kingma and Welling, 2014, Rezende et al., 2014, Burda et al., 2016], the resulting algorithm, AESMC, allows both the imposing of structure on the model, and the learning of an inference scheme that directly exploits this structure. Many previous approaches are explicitly or implicitly based on importance sampling inference which is known to scale poorly to high dimensions. By instead basing our inference on SMC, AESMC opens up many opportunities for carrying out model learning and inference amortization in higher dimensions and on a wider range of models.

2 Background

In this section, we review non-Markovian state-space models (SSMs), SMC and variational auto-encoders (VAEs). AESMC relies on the strengths of SMC in performing inference and VAEs in simultaneous model learning and amortized inference.

2.1 Non-Markovian State-Space Models

Although SMC can be used for an arbitrary series of targets [Naesseth et al., 2014, Wood et al., 2014], we will, for the most part, focus on the case of non-Markovian SSMs for simplicity.

SSMs are probabilistic models over a set of latent variables $X_t \in \mathcal{X}_t, \forall t = 1 : T$ and observed variables $Y_t \in \mathcal{Y}_t, \forall t = 1 : T$. We can further consider a model to be parameterized by $\theta \in \Theta$. The SSM is then characterized by an initial density $\mu_\theta(x_1)$, a series of transition densities $f_{t,\theta}(x_t|x_{1:t-1})$, and a series of emission densities $g_{t,\theta}(y_t|x_{1:t})$

$$\begin{aligned} X_1 &\sim \mu_\theta(\cdot), \\ X_t|(X_{1:t-1} = x_{1:t-1}) &\sim f_{t,\theta}(\cdot|x_{1:t-1}), \\ Y_t|(X_{1:t} = x_{1:t}) &\sim g_{t,\theta}(\cdot|x_{1:t}). \end{aligned}$$

The joint density of the SSM is then as follows

$$p_\theta(x_{1:T}, y_{1:T}) = \mu_\theta(x_1) \prod_{t=2}^T f_{t,\theta}(x_t|x_{1:t-1}) \prod_{t=1}^T g_{t,\theta}(y_t|x_{1:t}).$$

We are free to choose any density for $\mu_\theta(x_1)$ and each $f_{t,\theta}(x_t|x_{1:t-1})$ and $g_{t,\theta}(y_t|x_{1:t})$. One is usually interested characterizing the posterior

$$p_\theta(x_{1:T}|y_{1:T}) \propto p_\theta(x_{1:T}, y_{1:T})$$

or expectations of some function φ under this posterior

$$I(\varphi) = \int \varphi(x_{1:T}) p_\theta(x_{1:T}|y_{1:T}) dx_{1:T}$$

which can be used further in some decision-theoretic framework. We refer to these two tasks as inference. Inference in models which are non-linear, non-discrete, and non-Gaussian is difficult and one must resort to approximate methods, for which SMC has been shown to be one of the most successful approaches [Doucet and Johansen, 2009].

2.2 Sequential Monte Carlo

SMC exploits the structure of a model by breaking down the overall inference problem into a series of target distributions which get incrementally closer to the distribution of interest. These targets are

then approximated by propagating a population of samples known as particles. If each intermediary target is kept similar to its predecessor, approximating one target given the last forms a significantly simpler problem than the overall inference. Meanwhile, the information gained for approximating each successive target can be exploited to update the particle population, reallocating computational resources to more promising regions.

More formally, SMC performs approximate inference on a sequence of target distributions $(\pi_t(x_{1:t}))_{t=1}^T$ of increasing spaces $(\mathcal{X}_1 \times \dots \times \mathcal{X}_t)_{t=1}^T$. In the context of SSMS, the target distributions are often taken to be $(p_\theta(x_{1:t}|y_{1:t}))_{t=1}^T$. At each time step t , we have a set of K particles $(\tilde{x}_{1:t}^k)_{k=1}^K$, corresponding to samples of the latents, and respective particle weights $(w_t^k)_{k=1}^K$. Using these weighted particles, one can approximate each posterior $p_\theta(x_{1:t}|y_{1:t})$. In particular, the posterior for the complete model $p_\theta(x_{1:T}|y_{1:T})$ and the expectation $I(\varphi)$ can be approximated using the following estimators

$$\hat{p}_\theta(x_{1:T}|y_{1:T}) = \sum_{k=1}^K \bar{w}_T^k \delta_{\tilde{x}_{1:T}^k}(x_{1:T}), \quad (1)$$

$$\hat{I}(\varphi) = \sum_{k=1}^K \bar{w}_T^k \varphi(\tilde{x}_{1:T}^k), \quad (2)$$

where $\bar{w}_T^k := w_T^k / \sum_j w_T^j$ is the normalized weight and δ_z is a Dirac measure centred on z . Furthermore, one can obtain an unbiased estimator of the marginal likelihood $p_\theta(y_{1:T})$ using the intermediary particle weights:

$$\hat{Z}_{\text{SMC}} := \prod_{t=1}^T \left[\frac{1}{K} \sum_{k=1}^K w_t^k \right]. \quad (3)$$

In the simplest version of the SMC algorithm, one must specify the proposal distributions $q_{1,\phi}(x_1|y_1)$, $q_{t,\phi}(x_t|y_{1:t}, x_{1:t-1})$ ($t = 2, \dots, T$) which we assume to be parameterized by ϕ . The algorithm then proceeds by sampling particle values from the proposals, computing their weights, and resampling as described in Algorithm 1. The resampling step is achieved by, at each time step $t = 2, \dots, T$, selecting the ancestor index a_{t-1}^k for the k th particle from a discrete distribution $\mathcal{F}(\cdot|\bar{w}_{t-1}^1, \dots, \bar{w}_{t-1}^K)$ over parent indices $\{1, \dots, K\}$ with probabilities equal to the normalized weights at the previous time step $(\bar{w}_{t-1}^1, \dots, \bar{w}_{t-1}^K)$. Douc and Cappé [2005] provide a comparison of numerous different schemes for sampling from $\mathcal{F}(\cdot|\bar{w}_{t-1}^1, \dots, \bar{w}_{t-1}^K)$ that reduce the variance of the SMC estimates compared with naïve multinomial resampling. Of these, we use systematic resampling in our experiments.

The sequential nature of SMC and the resampling step are crucial in making SMC scalable to large T . The former makes it easier to design efficient proposal distributions as each step need only target the next set of variables $x_t \in \mathcal{X}_t$. The resampling step then allows the algorithm to focus on promising particles in light of new observations, avoiding the exponential divergence between the weights of different samples that occurs for importance sampling as T increases. This can be demonstrated both empirically and theoretically [Del Moral, 2004, Chapter 9]. We refer the reader to the review by Doucet and Johansen [2009] for an in-depth treatment of SMC.

2.3 Variational Auto-Encoders

Given a dataset of observations $(y^{(n)})_{n=1}^N$, a generative model $p_\theta(x, y)$ and an inference network $q_\phi(x|y)$, VAE [Kingma and Welling, 2014] is a framework for jointly learning model parameters θ and inference network parameters ϕ . The prior $p(x)$ is usually independent of θ . The likelihood $p_\theta(y|x)$ is usually a neural network with weights θ mapping from x to parameters of the probability distribution of the observation y . The inference network $q_\phi(x|y)$ is usually a neural network with weights ϕ mapping from y to the parameters of the probability distribution of the latents x .

The VAE algorithm maximizes the empirical average of ELBOs with respect to both generative and inference network parameters:

$$\underset{\theta, \phi}{\text{maximize}} \left\{ \mathcal{J}(\theta, \phi) := \frac{1}{N} \sum_{n=1}^N \text{ELBO}(\theta, \phi, y^{(n)}) \right\}, \quad (4)$$

Algorithm 1: Sequential Monte Carlo

Data: observed values $y_{1:T}$, model parameters θ , proposal parameters ϕ

Result: particles $(\tilde{x}_{1:T}^k)_{k=1}^K$, weights $(w_T^k)_{k=1}^K$, marginal likelihood estimate \hat{Z}_{SMC}

begin

Sample $x_1^k \sim q_{1,\phi}(\cdot|y_1)$ for $k = 1, \dots, K$.
Compute and normalize weights:

$$w_1^k = \frac{\mu_\theta(x_1^k) g_{1,\theta}(y_1|x_1^k)}{q_{1,\phi}(x_1^k|y_1)}, \quad \bar{w}_1^k = \frac{w_1^k}{\sum_{\ell=1}^K w_1^\ell}.$$

Initialize particles: $\tilde{x}_1^k \leftarrow x_1^k$

for $t = 2, 3, \dots, T$ **do**

Sample $a_{t-1}^k \sim \mathcal{F}(\cdot|\bar{w}_{t-1}^1, \dots, \bar{w}_{t-1}^K)$.

Sample $x_t^k \sim q_{t,\phi}(\cdot|y_{1:t}, \tilde{x}_{1:t-1}^k)$.

Update particle set $\tilde{x}_{1:t}^k \leftarrow (\tilde{x}_{1:t-1}^k, x_t^k)$.

Compute and normalize weights:

$$w_t^k = \frac{f_{t,\theta}(x_t^k|\tilde{x}_{1:t-1}^k) g_{t,\theta}(y_t|\tilde{x}_{1:t}^k)}{q_{t,\phi}(x_t^k|y_{1:t}, \tilde{x}_{1:t-1}^k)}, \quad \bar{w}_t^k = \frac{w_t^k}{\sum_{\ell=1}^K w_t^\ell}.$$

Compute marginal likelihood: $\hat{Z}_{\text{SMC}} = \prod_{t=1}^T \frac{1}{K} \sum_{k=1}^K w_t^k$.

return particles $(\tilde{x}_{1:T}^k)_{k=1}^K$, weights $(w_T^k)_{k=1}^K$, marginal likelihood estimate \hat{Z}_{SMC}

where, for a given observation $y^{(n)}$, the ELBO is a lower bound on the log of the evidence $p_\theta(y^{(n)})$ which becomes tight when the Kullback-Leibler (KL) divergence from $q_\phi(x|y^{(n)})$ to $p_\theta(x|y^{(n)})$ is zero:

$$\text{ELBO}(\theta, \phi, y^{(n)}) := \int q_\phi(x|y^{(n)}) \left[\log p_\theta(x, y^{(n)}) - \log q_\phi(x|y^{(n)}) \right] dx \quad (5)$$

$$= \log p_\theta(y^{(n)}) - \text{KL} \left(q_\phi(x|y^{(n)}) \parallel p_\theta(x|y^{(n)}) \right) \leq \log p_\theta(y^{(n)}). \quad (6)$$

Intuitively this optimization problem simultaneously maximizes the evidence and minimizes the KL divergence between the variational posterior approximation and the true posterior over all observations in the dataset.

The optimization is performed using stochastic gradient ascent (SGA) [Robbins and Monro, 1951] where stochastic gradients can be obtained by taking gradients with respect to a mini-batch of the dataset and samples from $q_\phi(\cdot|y^{(n)})$.

Reparameterization trick To take gradients with respect to ϕ , we cannot use samples from $q_\phi(x|y^{(n)})$ directly because the computation graph induced by the sampler (which must be parameterized by ϕ) is cut off from the overall computation graph. One solution is to pick an auxiliary probability distribution $p_\epsilon(\cdot)$ and a reparameterization function $r_\phi(\epsilon, y^{(n)})$ such that a random variable generated by sampling from $p_\epsilon(\cdot)$ and passing through $r_\phi(\cdot, y^{(n)})$ is the same as a random variable generated from $q_\phi(\cdot|y^{(n)})$. A stochastic gradient is then obtained as:

$$\nabla_{\theta, \phi} \left[\log p_\theta(r_\phi(\epsilon, y^{(n)}), y^{(n)}) - \log q_\phi(r_\phi(\epsilon, y^{(n)})|y^{(n)}) \right], \quad \epsilon \sim p_\epsilon(\cdot). \quad (7)$$

Importance Weighted Auto-Encoders Burda et al. [2016] extended VAEs by making a connection to importance sampling in a method they call importance weighted auto-encoder (IWAE). In particular, the objective function is

$$\underset{\theta, \phi}{\text{maximize}} \left\{ \mathcal{J}_{\text{IS}}(\theta, \phi) := \frac{1}{N} \sum_{n=1}^N \text{ELBO}_{\text{IS}}(\theta, \phi, y^{(n)}) \right\}, \quad (8)$$

where, for a given observation $y^{(n)}$, the ELBO_{IS} (with K particles) is a lower bound on the log of the evidence $p_\theta(y^{(n)})$ by Jensen's inequality:

$$\text{ELBO}_{\text{IS}}(\theta, \phi, y^{(n)}) := \int \left(\prod_{k=1}^K q_\phi(x^k | y^{(n)}) \right) \log \left(\sum_{k=1}^K \frac{p_\theta(x^k, y^{(n)})}{q_\phi(x^k | y^{(n)})} \right) dx^{1:K} \leq \log p_\theta(y^{(n)}). \quad (9)$$

Note that for $K = 1$, this reduces to the VAE framework. It can be shown that the bound is tighter for larger K .

3 Model Learning

In this section, we describe differentiating through SMC (∇_{SMC}), our approach to model learning based on maximizing the marginal likelihood $p_\theta(y_{1:T})$ of a model with respect to its parameters θ .

3.1 Differentiating through SMC

The marginal likelihood estimate \hat{Z}_{SMC} is a random variable whose randomness derives entirely from the particles generated stochastically by SMC. In particular, it depends on the values x_t^k proposed by q_t and the ancestors a_{t-1}^k which are drawn from \mathcal{F} . We can think of SMC as being a sampler for $(x_{1:T}^{1:K}, a_{1:T-1}^{1:K})$ with the density:

$$Q_{\text{SMC}}(x_{1:T}^{1:K}, a_{1:T-1}^{1:K}) := \left(\prod_{k=1}^K q_{1,\phi}(x_1^k) \right) \left(\prod_{t=2}^T \prod_{k=1}^K q_{t,\phi}(x_t^k | y_{1:t}, \tilde{x}_{1:t-1}^{a_{t-1}^k}) \right) \left(\prod_{t=1}^{T-1} \prod_{k=1}^K \frac{w_t^{a_t^k}}{\sum_{\ell=1}^K w_t^\ell} \right). \quad (10)$$

The key insight is that given a fixed realization of $(x_{1:T}^{1:K}, a_{1:T-1}^{1:K})$, Algorithm 1 is fully deterministic [Jin et al., 2017]. As long as this sample is distributed according to Q_{SMC} , the marginal likelihood estimate $\hat{Z}_{\text{SMC}}(y_{1:T}, \theta)$ will be unbiased [Del Moral, 2004], i.e. $\mathbb{E}[\hat{Z}_{\text{SMC}}(y_{1:T}, \theta)] = p_\theta(y_{1:T})$. Thus we can consider the SMC algorithm being run in two parts: one for generating a sample $(x_{1:T}^{1:K}, a_{1:T-1}^{1:K})$ and one for evaluating \hat{Z}_{SMC} deterministically using this sample. We can apply reverse-mode automatic differentiation (AD) on the deterministic computation graph to obtain the gradient $\nabla_\theta \hat{Z}_{\text{SMC}}$ which is, due to the Leibniz integral rule, an unbiased estimate of $\nabla p_\theta(y_{1:T})$:

$$\mathbb{E}[\nabla_\theta \hat{Z}_{\text{SMC}}] = \nabla_\theta \mathbb{E}[\hat{Z}_{\text{SMC}}] = \nabla_\theta p_\theta(y_{1:T}), \quad (11)$$

and hence can be used in an SGA algorithm. Note that in practice, we only need to run SMC once, sampling and building the deterministic computation graph simultaneously.

This procedure is valid provided that the random variable $(x_{1:T}^{1:K}, a_{1:T-1}^{1:K})$ is not parameterized by θ . When this condition does not hold, one can use gradient estimation methods [Schulman et al., 2015] such as the reparameterization trick [Kingma and Welling, 2014] or the reinforce trick [Williams, 1992]. We summarize the ∇_{SMC} algorithm for model learning in Algorithm 2.

Algorithm 2: ∇_{SMC}

Data: observed values $y_{1:T}$, generative model p_θ , number of particles K

Result: learned model parameters θ^*

begin

 Initialize θ^*

while *not converged* **do**

$x_{1:T}^{1:K}, a_{1:T-1}^{1:K} \leftarrow$ Run SMC forward

$g_\theta \leftarrow$ Evaluate gradient estimator $\nabla_\theta \log \hat{Z}_{\text{SMC}}$ by running reverse-mode AD

$\theta^* \leftarrow$ Perform SGA step using g_θ

return θ^*

3.2 Proposal Distributions

It is well known that the choice of proposal distributions is crucial for the performance of SMC through the variance of the particle weights and consequently the variance of the marginal likelihood estimate. It can be shown for a given series of target distributions, the optimal proposals (in terms of minimizing the one-step weight variance) is $q_{t,\phi}(x_t|y_{1:t}, x_{1:t-1}) = p_\theta(x_t|y_{1:t}, x_{1:t-1})$ [Doucet and Johansen, 2009, Section 4.1]. In most cases $p_\theta(x_t|y_{1:t}, x_{1:t-1})$ is intractable and impossible to sample from directly.

Although methods for adapting SMC proposals to approximate $p_\theta(x_t|y_{1:t}, x_{1:t-1})$ exist [Gu et al., 2015, Paige and Wood, 2016], the most commonly used choice is to set $q_{t,\phi}(x_t|y_{1:t}, x_{1:t-1})$ to the transition distribution $f_{t,\theta}(x_t|x_{1:t-1})$, known as the bootstrap proposal. This simplifies the calculation of the weight w_t^k to just calculating the emission density $g_{t,\theta}(y_t|x_{1:t}^k)$.

We will therefore consider two types of proposals for ∇ SMC. First, we will consider proposals $q_{t,\phi}(x_t|x_{1:t-1})$ that are independent of θ . The use of this proposal in Algorithm 2 is straightforward. Second, we will consider the bootstrap proposal $f_{t,\theta}(x_t|x_{1:t-1})$ which we now discuss in depth.

3.2.1 Using the Bootstrap Proposal

On the surface it appears using a bootstrap proposal violates the requirement that $(x_{1:T}^{1:K}, a_{1:T-1}^{1:K})$ is not parametrized by θ . Indeed this would be the case for a naïve approach as one typically cancels the transition and proposal terms in the weight calculation, $w_t^k = g_{t,\theta}(y_t|\tilde{x}_{1:t}^k)$, when using the bootstrap proposal. This would mean that the transition distribution $f_{t,\theta}$ would not feature in the optimization target. However, we can instead consider treating the proposal as fixed, but instantaneously equal to the transition distribution. In other words, we maintain a symbolic distinction between θ and ϕ giving

$$\begin{aligned}\nabla_\theta w_t^k &= \nabla_\theta \frac{f_{t,\theta}(x_t^k|\tilde{x}_{1:t-1}^{a_{t-1}^k})g_{t,\theta}(y_t|\tilde{x}_{1:t}^k)}{q_{t,\phi}(x_t^k|y_{1:t}, \tilde{x}_{1:t-1}^{a_{t-1}^k})} \\ &= \frac{1}{q_{t,\phi}(x_t^k|y_{1:t}, \tilde{x}_{1:t-1}^{a_{t-1}^k})} \nabla_\theta \left[f_{t,\theta}(x_t^k|\tilde{x}_{1:t-1}^{a_{t-1}^k})g_{t,\theta}(y_t|\tilde{x}_{1:t}^k) \right],\end{aligned}$$

and then make the choice of setting $\phi_i = \hat{\theta}_i$ at optimization iteration i where $\hat{\theta}_i$ is the model parameters used at that iteration. Each ϕ_i is now just a fixed value, chosen to coincide with the current model estimate. Since we are taking ϕ to have the same value as θ but treating it as a different variable symbolically, we consider the random variable $(x_{1:T}^{1:K}, a_{1:T-1}^{1:K})$ to be parameterized by ϕ . Noting that as the marginal likelihood estimate is unbiased for any choice of ϕ and so does not affect the target, we can still perform the SGA update by taking the derivative $\nabla_\theta \hat{Z}_{\text{SMC}}$ for a sample of $(x_{1:T}^{1:K}, a_{1:T-1}^{1:K})$.

3.3 Variance Issues

Unfortunately the variance in the estimate for \hat{Z}_{SMC} can be very high if one is unable to use sufficient particles in the SMC sweep. This is an inevitable consequence of the challenging nature of Bayesian inference, noting that calculating $p_\theta(y_{1:T})$ corresponds to calculation of a high dimensional inference. Furthermore, although \hat{Z}_{SMC} is unbiased, its distribution tends to have significant positive skew. Both of these can significantly diminish the performance of the SGA algorithm if using $\nabla_\theta \hat{Z}_{\text{SMC}}$ directly.

The log marginal likelihood estimator $\log \hat{Z}_{\text{SMC}}$ is on the other hand is significantly more stable, having a far lower variance and typically significantly less skew [Bérard et al., 2014]. Although SMC produces (negatively) biased estimates for $\log p_\theta(y_{1:T})$, it can be shown [Bérard et al., 2014] that this bias is reduced as we use more particles, tending to zero in the limit $K \rightarrow \infty$. As we found that in practise the effect of this bias is negligible, compared to the gains from the reduction in variance we used in our experiments $\nabla_\theta \log \hat{Z}_{\text{SMC}}$ as the stochastic gradient to optimize $\mathbb{E}[\log \hat{Z}_{\text{SMC}}]$, which is, due to the Jensen's inequality a lower bound on $\log p_\theta(y_{1:T})$.

4 Auto-Encoding Sequential Monte Carlo

In this section, we will present two extensions to ∇SMC . First, we present a method for doing simultaneous model learning and proposal adaptation given a single sequence of observations $y_{1:T}$. Second, we present AESMC, a method for model learning and amortizing proposal distributions over a dataset of observations $(y_{1:T}^{(n)})_{n=1}^N$ and relate it to VAEs [Kingma and Welling, 2014].

4.1 Model Learning and Proposal Adaptation

Similarly to case of ∇SMC , we use $p_\theta(x_{1:T}, y_{1:T})$ to denote the family of generative models over latent variables $x_{1:T}$ and observed variables $y_{1:T}$. The learnable parameters θ can be weights of a *generative network*. The proposal distributions are parameterized by the output of a *proposal network*. Let us use $q_\phi(x_{1:T}|y_{1:T})$ to denote the joint proposal distribution.

The main difference with ∇SMC is that we not only want to learn the model, we also want to learn adapted SMC proposals that provide effective inference in the learnt models.

Generative Network The generative network is a set of functions in the generative model parameterized by θ that we want to learn. We require that $f_{t,\theta}(x_t|x_{1:t-1})$ and $g_{t,\theta}(y_t|x_{1:t})$ are differentiable with respect to θ .

This formulation allows us to learn generative models from a broad range of families with varying degrees of structure. On the one end, we can perform parameter estimation where a small number parameters are to be learned. On the other end, we can substitute a large part of the transition $f_{t,\theta}(x_t|x_{1:t-1})$ (similarly the emission $g_{t,\theta}(y_t|x_{1:t})$) by a neural network, for example one which takes $x_{1:t-1}$ as input and outputs parameters of a distribution of x_t . Here, the parameters θ correspond to the neural network weights.

Proposal Network The proposal network is a set of functions in the joint proposal $q_\phi(x_{1:T}|y_{1:T})$ parameterized by ϕ that we want to learn. This is also known as an inference network. A particular factorization of $q_\phi(x_{1:T}|y_{1:T})$ will guide the architecture of the proposal network. For instance, for the factorization

$$q_\phi(x_{1:T}|y_{1:T}) = q_{t,\phi}(x_1|y_1) \prod_{t=2}^T q_{t,\phi}(x_t|x_{1:t-1}, y_{1:t}), \quad (12)$$

we could choose the proposal network to be a long short-term memory (LSTM) [Hochreiter and Schmidhuber, 1997] which at each time t takes as input a combination of x_{t-1} and y_t and outputs parameters of a distribution of x_t . By virtue of maintaining an internal cell, the LSTM will respect the factorization in (12). The family of proposal networks parameterized by ϕ should be general enough to encapsulate the optimal proposal better than naïve proposals for a correctly chosen ϕ .

For generative network and proposal network architectures used in this work, refer to Appendix B.

Objective Function Our objective function should encapsulate the two goals that we are trying to achieve: learn a model and adapt SMC proposals. We have shown in (6) that $\text{ELBO}(\theta, \phi, y_{1:T})$ in (5) is a lower bound of $\log p_\theta(y_{1:T})$ with the gap being $\text{KL}(q_\phi(x_{1:T}|y_{1:T})||p_\theta(x_{1:T}|y_{1:T}))$. Thus, we can interpret maximizing $\text{ELBO}(\theta, \phi, y_{1:T})$ with respect to (θ, ϕ) as searching for (θ, ϕ) that maximizes $\log p_\theta(y_{1:T})$ and minimizes $\text{KL}(q_\phi(x_{1:T}|y_{1:T})||p_\theta(x_{1:T}|y_{1:T}))$. This can be interpreted as simultaneously learning the model and finding a good variational posterior approximation.

In the case of maximizing $\text{ELBO}_{\text{IS}}(\theta, \phi, y_{1:T})$ in (9), we derive (see Appendix A.2) a closed form expression for the gap between $\text{ELBO}_{\text{IS}}(\theta, \phi, y_{1:T})$ and $\log p_\theta(y_{1:T})$ that was not present in the original paper by Burda et al. [2016]:

$$\text{KL} \left(\prod_{k=1}^K q_\phi(x_{1:T}^k|y_{1:T}) \middle| \middle| \frac{1}{K} \sum_{k=1}^K \frac{\prod_{\ell=1}^K q_\phi(x_{1:T}^\ell|y_{1:T})}{q_\phi(x_{1:T}^k|y_{1:T})} p_\theta(x_{1:T}^k|y_{1:T}) \right). \quad (13)$$

This allows IWAE to be interpreted as an algorithm that performs simultaneous model learning and importance sampling (IS) proposal adaptation. This can be seen from the fact that the KL divergence in (13) being zero implies $q_\phi(x_{1:T}^k|y_{1:T}) = p_\theta(x_{1:T}^k|y_{1:T})$.

Let us denote our proposed objective $\text{ELBO}_{\text{SMC}}(\theta, \phi, y_{1:T})$ and define it to be the expectation of the log of the SMC based evidence estimator:

$$\text{ELBO}_{\text{SMC}}(\theta, \phi, y_{1:T}) := \mathbb{E} \left[\log \hat{Z}_{\text{SMC}} \right] = \mathbb{E} \left[\log \prod_{t=1}^T \frac{1}{K} \sum_{k=1}^K \frac{f_{\theta}(x_t^k | \hat{x}_{1:t-1}^{a_{t-1}^k}) g_{\theta}(y_t | \hat{x}_{1:t}^k)}{q_{t,\phi}(x_t^k | y_{1:t}, \hat{x}_{1:t-1}^{a_{t-1}^k})} \right], \quad (14)$$

where the expectation is under the sampling distribution Q_{SMC} of SMC as shown in (10). We want to maximize this quantity with respect to θ and ϕ .

We derive a closed form expression for the gap between $\text{ELBO}_{\text{SMC}}(\theta, \phi, y_{1:T})$ and $\log p_{\theta}(y_{1:T})$ (see Appendix A.3) as:

$$\text{KL} \left(Q_{\text{SMC}}(x_{1:T}^{1:K}, a_{1:T-1}^{1:K}) \left\| \frac{Q_{\text{SMC}}(x_{1:T}^{1:K}, a_{1:T-1}^{1:K}) \hat{Z}_{\text{SMC}}}{p_{\theta}(y_{1:T})} \right\| \right). \quad (15)$$

Note that since \hat{Z}_{SMC} is a function of $(x_{1:T}^{1:K}, a_{1:T-1}^{1:K})$, (15) being zero implies that \hat{Z}_{SMC} is a zero variance (and unbiased) estimator of $p_{\theta}(y_{1:T})$. Therefore, we can interpret maximizing $\text{ELBO}_{\text{SMC}}(\theta, \phi, y_{1:T})$ as simultaneously learning the model and adapting the proposal distribution q_{ϕ} in the sense of simultaneously maximizing $p_{\theta}(y_{1:T})$ and minimizing the variance of \hat{Z}_{SMC} . We consider this more formally in Appendix A.3.

Differentiating through Resampling To estimate the partial gradient of ELBO_{SMC} in (14) with respect to θ , we can use a method similar to ∇_{SMC} since the sampling distribution of the expectation is independent of θ . To estimate the partial gradient of ELBO_{SMC} in (14) with respect to ϕ , we can analytically obtain

$$\int \left[(\nabla_{\phi} \log Q_{\text{SMC}}(x_{1:T}^{1:K}, a_{1:T-1}^{1:K})) \log \hat{Z}_{\text{SMC}} + \nabla_{\phi} \log \hat{Z}_{\text{SMC}} \right] Q_{\text{SMC}}(x_{1:T}^{1:K}, a_{1:T-1}^{1:K}) dx_{1:T}^{1:K} da_{1:T-1}^{1:K}. \quad (16)$$

Hence we can use $\left[(\nabla_{\phi} \log Q_{\text{SMC}}(x_{1:T}^{1:K}, a_{1:T-1}^{1:K})) \log \hat{Z}_{\text{SMC}} + \nabla_{\phi} \log \hat{Z}_{\text{SMC}} \right]$ as an unbiased estimator of the gradient.

Empirically, we find that the proposal network that arises from not accounting for the resampling step and following a biased gradient still outperforms previous approaches. To reduce the bias, we additionally reparameterize sampling of $x_{1:T}^{1:K}$ when it is possible. In particular, noting that \hat{Z}_{SMC} is a function of $(x_{1:T}^{1:K}, a_{1:T-1}^{1:K}, \theta, \phi)$, we use the gradient estimator

$$\nabla_{\phi} \log \hat{Z}_{\text{SMC}}(r_{\phi}(\epsilon_{1:T}^{1:K}, y_{1:T}), a_{1:T-1}^{1:K}, \theta, \phi), \quad \epsilon_{1:T}^{1:K} \sim p_{\epsilon_{1:T}^{1:K}}(\cdot), \quad (17)$$

where $\epsilon_{1:T}^{1:K}$ are random variables independent of ϕ , and r_{ϕ} is a reparameterization function for which it holds that a random variable sampled from $p_{\epsilon_{1:T}^{1:K}}(\cdot)$ and passed through $r_{\phi}(\cdot, y_{1:T})$ results in the same random variable as one sampled from $q_{\phi}(\cdot | y_{1:T})$.

Stochastic Gradient Optimization We optimize the objective using an SGA algorithm. In particular, we run SMC as described in Algorithm 1 forward, simultaneously sampling from Q_{SMC} and building a deterministic computation graph. In the backward pass, we obtain unbiased gradients of ELBO_{SMC} and perform a parameter update step.

4.2 AESMC: Model Learning and Proposal Amortization

Up until now, we were concerned with learning the model and adapting proposals one sequence of observations $y_{1:T}$. Now, we consider the case when we are given a dataset of observations $(y_{1:T}^{(n)})_{n=1}^N$ from the true distribution $p_{\theta^*}(y_{1:T})$ where θ^* is the underlying parameter θ .

Model learning will here be understood as maximizing $\frac{1}{N} \sum_{n=1}^N \log p_{\theta}(y_{1:T}^{(n)})$ with respect to θ . Proposal amortization in this case refers to reducing the cost of inference on a new observation sequence $y_{1:T}^{\text{new}} \sim p_{\theta^*}(y_{1:T})$ by learning a proposal network that is able to map from $y_{1:T}^{\text{new}}$ to parameters of adapted proposal distribution for $y_{1:T}^{\text{new}}$.

To reflect amortization, we simply set the objective function that we want to maximize to the empirical average of $\text{ELBO}_{\text{SMC}}(\theta, \phi, y^{(n)})$ over all data points:

$$\max_{\theta, \phi} \left\{ \mathcal{J}_{\text{SMC}}(\theta, \phi) := \frac{1}{N} \sum_{n=1}^N \text{ELBO}_{\text{SMC}}(\theta, \phi, y_{1:T}^{(n)}) \right\}. \quad (18)$$

Given results in Section 4.1, \mathcal{J}_{SMC} simply decomposes to two terms one of which learns the model and another adapts proposal distributions for the whole dataset.

The optimization is performed using SGA and differentiation through the resampling step is handled in a similar manner to the procedure in Section 4.1. Note that since number of observation sequences N can be large, we perform double SGA: one for sampling observation sequences from the dataset¹, one for estimating ELBO_{SMC} . To summarize, we obtain a procedure for simultaneous model learning and proposal amortization as outlined in Algorithm 3.

Algorithm 3: Auto-encoding sequential Monte Carlo

Data: observed values $y_{1:T}$, generative network p_θ , proposal network q_ϕ , number of particles K

Result: optimized parameters θ^*, ϕ^*

begin

 Initialize θ^*, ϕ^*

while not converged **do**

for n in $\{1, \dots, N\}$ **do**

$y_{1:T} \leftarrow$ Sample uniformly from $(y_{1:T}^{(n)})_{n=1}^N$

$x_{1:T}^{1:K}, a_{1:T-1}^{1:K} \leftarrow$ Run SMC forward

$g_\theta \leftarrow$ Evaluate gradient estimator $\nabla_\theta \log \hat{Z}_{\text{SMC}}$ by running reverse-mode AD

$g_\phi \leftarrow$ Evaluate gradient estimator

$\left[(\nabla_\phi \log Q_{\text{SMC}}(x_{1:T}^{1:K}, a_{1:T-1}^{1:K})) \log \hat{Z}_{\text{SMC}} + \nabla_\phi \log \hat{Z}_{\text{SMC}} \right]$ by running reverse-mode AD

$\theta^*, \phi^* \leftarrow$ Perform SGA step using g_θ, g_ϕ

return θ^*, ϕ^*

5 Experiments

The following experiments serve to empirically validate ∇SMC and AESMC.

To validate ∇SMC , we first consider a one dimensional non-linear state space model and look at the variance of our gradient estimates compared to alternatives approaches, along with examining the convergence of the parameters and marginal likelihood estimate. We then consider a higher dimensional state space model, where we learn the parameter of a linear transition function, demonstrating that ∇SMC is capable of performing model learning in higher dimensional parameter spaces.

To validate AESMC, we compare the optimization of \mathcal{J}_{IS} and \mathcal{J}_{SMC} in equations (8) and (18) on three various datasets. First, we consider the *Polyphonic Music* dataset introduced by Boulanger-Lewandowski et al. [2012] which consists of unsupervised sequences of $\{0, 1\}^{88}$ vectors. Second, we consider the *Moving MNIST* dataset introduced by Srivastava et al. [2015] which consists of sequences of 64×64 frames of moving MNIST digits [LeCun, 1998]. Third, we introduce a dataset that we call *Moving Agents* of moving objects similar to the *Moving Balls* dataset introduced by Ondruška and Posner [2016]. The objects are circular cylinders with bases touching a 2D plane but are only observed through a LIDAR-like view which can lead to occasional occlusion of one object by another. The crucial difference is that the moving objects here have stochastic policies that are dependent on the state of the other objects.

¹In practice, we perform minibatch SGA.

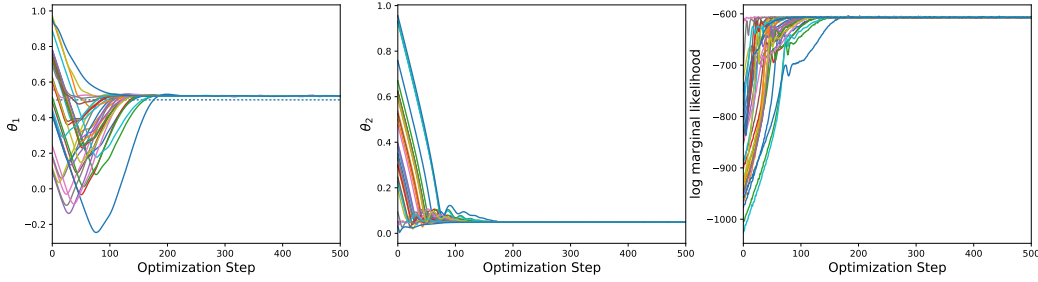


Figure 1: θ_1 , θ_2 and log likelihood convergence plot from 30 randomly initialized runs of a non-linear state space model.

5.1 Non-linear State Space Model

We consider a benchmark non-linear state space model from [Andrieu et al. \[2010\]](#), amongst others, with one dimensional state and observation spaces denoted by $X_t \in \mathbb{R}$ and $Y_t \in \mathbb{R}$ respectively. The model is defined by two unknown parameters $\theta_1, \theta_2 \in \mathbb{R}$, where θ_1 affects the transition dynamics and θ_2 affects the observation dynamics. The full model is given by

$$X_1 \sim \mathcal{N}(0, \sqrt{5}^2) \quad (19)$$

$$X_t = \theta_1 X_{t-1} + \frac{25X_{t-1}}{1 + X_{t-1}^2} + 8\sqrt{10} \cos(1.2t) + U_t \quad (20)$$

$$Y_t = \theta_2 X_t^2 + \sqrt{10}V_t. \quad (21)$$

Each U_t and V_t are independent unit random normal variables. Here the non-linear nature of the transition dynamics prevents calculation of an analytic solution, while the multi-modal nature of the latent space makes inference challenging for long state sequences or when the parameters are unknown.

We generated synthetic data by using the above equations to generate a random sequence of 200 observations, $y_{t=1:200}$, with parameters $\theta_1 = 0.5$ and $\theta_2 = 0.05$. Given this data, we first carried out ∇ SMC using 10^5 particles and fixed proposal distributions $x_t \sim \mathcal{N}(x_{t-1}, 20^2)$, i.e. Gaussians centered at the previous latent value with a standard deviation of 20. Adam [[Kingma and Ba, 2014](#)] was used for the SGA, with the learning rate reduced linearly from 0.01 at the first iteration to 0.001 by the 500th optimization step and all other parameters set to their default values.

The convergence of ∇ SMC for this problem is shown in Figure 1. We can see that the parameters quickly converge to values very close to those used to generate the data, while the marginal likelihood estimate quickly increases to the same steady value across runs. The average marginal likelihood estimate achieved by these runs at the last optimization step was equal to -606.50 which almost exactly matches an estimated marginal likelihood of -606.73 for the parameters used to generate the data. This estimate was found by combining a number of SMC sweeps with those model parameters fixed.

To further investigate the performance of ∇ SMC and provide comparisons to possible alternative, we now consider the empirical variance of our gradient estimates. Here we compare to three possible alternatives. Firstly, we consider calculating marginal likelihood estimates from importance sampling, with gradients again calculated using AD of a computation graph². We refer to this approach as ∇ IS.

Secondly we consider calculating the gradients using the finite difference method introduced by [Poyiadjis et al. \[2006\]](#) based on simultaneous perturbation stochastic approximation (SPSA) [[Spall, 1992](#)]. This method samples perturbations $\Delta_d \sim \text{Bernoulli}$, $\forall d = 1, \dots, D$ where D is the dimensionality of θ and calculates log marginal likelihood estimates at $\theta^+ = \theta + \varepsilon_{1:D} \odot \Delta_{1:D}$ and $\theta^- = \theta - \varepsilon_{1:D} \odot \Delta_{1:D}$ using SMC where \odot represents an element-wise product and $\varepsilon_{1:D}$ is a vector of step sizes for the

²Note that the computation graph for importance sampling is slightly different to that for SMC.

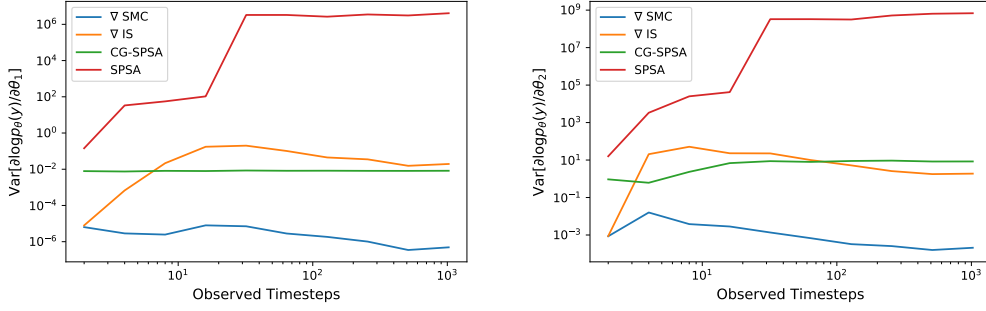


Figure 2: Empirical variance of the likelihood gradient with respect to θ_1 (left) and θ_2 (right) for different values of T in the non-linear state space model. Variance estimates are calculated using 100 independent inference sweeps.

finite difference calculation. The gradient estimate in direction d is then given by

$$\frac{\partial \log \widehat{p_\theta}(y_{1:T})}{\partial \theta_d} = \frac{\log \hat{p}_{\theta+}(y_{1:T}) - \log \hat{p}_{\theta-}(y_{1:T})}{2\epsilon_d \Delta_d}.$$

To reduce the variance, the method fixes the random number seed to the same value when calculating each SMC sweep, but because of the resampling, the samples of the latent variables will still vary between the two runs.

Finally we consider using the same SPSA algorithm, but as an alternative to AD for calculating derivatives of Algorithm 1 given the raw SMC outputs. We denote this method computational graph SPSA (CG-SPSA) due to sharing the same computation graph as ∇ SMC.

For all four methods, we estimated the variance in derivatives $\mathbb{V}[\nabla_\theta \log p_\theta(y_{1:t})]$ at the point $\theta_1 = \theta_2 = 1$ for data generated with parameter values $\theta_1^* = 0.5$ and $\theta_2^* = 0.05$ and for different length state sequences (between $T = 1$ and $T = 1024$). For each length T , the variance was estimated empirically using 100 independent inference sweeps. For the finite difference methods, we set $\epsilon_{1:D} = (0.1, 0.01)$.

Figure 2 shows the corresponding variance estimates as a function of state sequence length. We see that ∇ SMC clearly outperforms the other methods, producing gradient estimates that are orders of magnitude lower (except for very short sequences for which importance sampling is still reasonable). SPSA performs particularly poorly, producing large variance estimates at all lengths. The significantly better performance of CG-SPSA than SPSA highlights the gains of our computational graph approach and underlines why this is an essential component in the ability of ∇ SMC to perform model learning effectively. Furthermore, the improvements of ∇ SMC over CG-SPSA shows the importance of using an exact gradient method, such as AD, as opposed to approximate finite difference methods.

∇ SMC also provides speed advantages over the finite difference based models as it does not require multiple SMC runs. Over a sequence of 1024 observed states ∇ SMC required 6.80sec/iter, ∇ IS 3.61sec/iter, CG-SPSA 8.99sec/iter, and SPSA 13.46sec/iter.

Although importance sampling alleviates the problem of discontinuities arising from the resampling in SMC, it typically has far higher variances in the marginal likelihood estimates. We see that this high variance in the marginal likelihood estimates (increasing with T), translate to high variances in the gradient estimates for ∇ IS, compared with ∇ SMC. A slightly surprising result is that these variances reduce with T for ∇ IS above around $T = 10$. This is presumably because the parameters are shared between time steps, such that a longer sequences provides more information for the gradient calculation.

5.2 High-dimensional Linear State Space Model

For the next experiment we consider a variation of the multivariate linear Gaussian model reviewed by Roweis and Ghahramani [1999]. The latent state X_t in our model is a seven dimensional vector that is perturbed by a transformation matrix and elementwise Gaussian noise at each time step. The

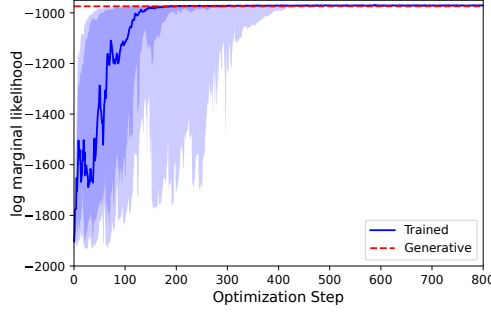


Figure 3: Learning the transition parameter A in an SSM with Student’s t emissions with ∇ SMC with bootstrap proposals and 10000 particles given a synthetic sequence of observations $y_{1:T}$ generated from the true model with $T = 250$. The log marginal likelihood of the generative parameters is estimated using repeated independent SMC with $10k$ particles with bootstrap proposals in the *true* model. The plot shows the empirical median, inter quartile range and inter decile range of the log marginal likelihood during optimization for 30 independent runs.

observed state Y_t is produced by compressing X_t into two dimensions with another unknown matrix and Student t noise. Specifically our model is defined as

$$X_1 \sim \mathcal{N}(0, I) \quad (22)$$

$$X_t = AX_{t-1} + \epsilon_t, \quad t = 1, \dots, T \quad (23)$$

$$Y_t = CX_t + \nu_t, \quad t = 1 \dots, T \quad (24)$$

where $(\epsilon_t)_{t=1}^T$ is a sequence of seven dimensional vectors of independent standard normal random variables; $(\nu_t)_{t=1}^T$ is a sequence of two dimensional vectors where each value is independently drawn from a Student’s t distribution with 5 degrees of freedom; A is an unknown 7×7 transition matrix; and C is a fixed 2×7 matrix.

Data was generated by sampling a ground truth A as random rotation matrix with a 0.99 scaling factor to ensure the latent process is bounded. Using the Gram-Schmidt orthonormalization procedure random matrices are mapped onto the space of rotation matrices without blocking gradients. The matrix C is presumed to be known and was generated by drawing each row from a seven-dimensional Dirichlet symmetric distribution with the concentration parameter 0.2. Again our task is to learn the best model, in this case the transformation matrix A , to explain the data within a family of models without access to the latent state. Using this A and C , observations for 250 time steps $y_{1:250}$ were generated. Using this data, we carried out ∇ SMC with 10000 particles and taking a bootstrap proposal. The initial learning rate was set to 1.0 and decayed polynomially to 0.1 over 1000 training iterations.

Figure 3 demonstrates that it is possible to use ∇ SMC in a setting where the number of parameters to be learned is high to learn a model as likely as the original. This constitutes a significant improvement in this respect over approaches for simultaneous optimization and inference based on Bayesian optimization such as the one by Rainforth et al. [2016a] in which the dimensionality of the parameters to be learned must be less than around 20. Moreover, this experiment demonstrates that ∇ SMC can in principle be applied in a model learning context where parts of the model are deep neural networks and parameters to be learned are the neural network weights.

5.3 Polyphonic Music

In this experiment, we consider the *Polyphonic Music* dataset introduced by Boulanger-Lewandowski et al. [2012]. This dataset consists of four different types of sequences of polyphonic music: JSB Chorales, Piano-midi.de, Nottingham and MuseData. Each dataset type consists of N unlabeled sequences $(y_{1:T_n}^{(n)})_{n=1}^N$ of varying lengths T_n where $y_t^{(n)} \in \{0, 1\}^{88}$. We focus on JSB Chorales for which $N = 229$ and T_n varies between 25 and 129. For the test set, $N = 77$ and T_n varies between 32 and 160.

For a fixed generative network architecture for $f_{t,\theta}$ and $g_{t,\theta}$ and proposal network architecture $q_{t,\phi}$, we compare test performance of IWAE and AESMC. Since each observation sequence has a different length, we train and test on the normalized objective:

$$\bar{\mathcal{J}}_{\text{IS}} := \frac{1}{N} \sum_{n=1}^N \left(\frac{1}{T_n} \text{ELBO}_{\text{IS}}(\theta, \phi, y_{1:T_n}^{(n)}) \right), \bar{\mathcal{J}}_{\text{SMC}} := \frac{1}{N} \sum_{n=1}^N \left(\frac{1}{T_n} \text{ELBO}_{\text{SMC}}(\theta, \phi, y_{1:T_n}^{(n)}) \right). \quad (25)$$

For the architecture, we use the one introduced by [Krishnan et al. \[2017\]](#). The transition is based on a gated recurrent unit (GRU) [\[Chung et al., 2015\]](#). Emission is a multilayer perceptron (MLP) mapping to probabilities of independent Bernoulli distributions on y_t . The proposal network is a right-to-left LSTM taking in the sequence of observations $y_{t:T}$ and at time t combining the LSTM output at that time with the previous state x_{t-1} to obtain the current mean and variances of a multivariate, diagonal covariance, normal distribution. Dimensionality of the latent variable is 100.

We train either using $\bar{\mathcal{J}}_{\text{IS}}$ or $\bar{\mathcal{J}}_{\text{SMC}}$ with number of particles in $\{5, 10, 20\}$ and report the corresponding objective evaluated on 100 test sequences with $K = 20$ particles. We used ADAM with the learning rate 1×10^{-3} . The left plot in Figure 4 demonstrates that AESMC converges faster than IWAE.

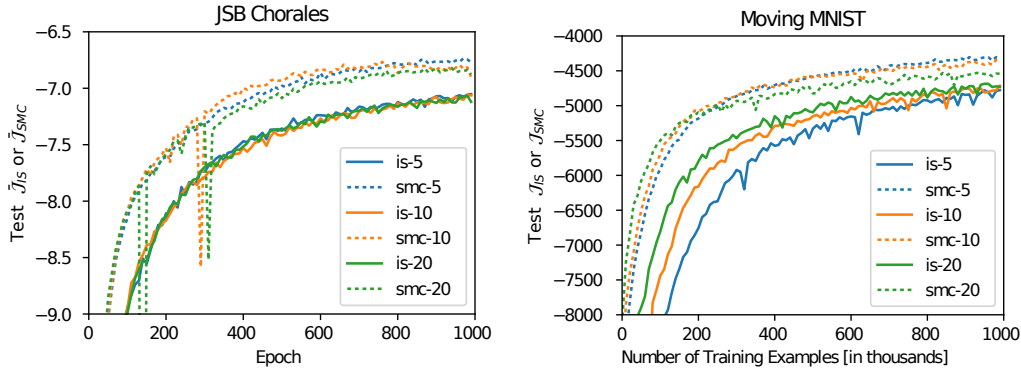


Figure 4: Simultaneous model learning and proposal amortization using IWAE and AESMC. In the legend, “is” corresponds to training with IWAE and “smc” to training with AESMC; suffix numbers correspond to number of particles K used in training. (left) JSB Chorales (Polyphonic Music) dataset [\[Boulanger-Lewandowski et al., 2012\]](#). The vertical axis shows the value of either $\bar{\mathcal{J}}_{\text{IS}}$ (if trained with IWAE) or $\bar{\mathcal{J}}_{\text{SMC}}$ (if trained with AESMC) evaluated on the JSB Chorales test dataset with number of particles $K = 20$. (right) Moving MNIST dataset [\[Srivastava et al., 2015\]](#). The vertical axis shows the value of either $\bar{\mathcal{J}}_{\text{IS}}$ (if trained with IWAE) or $\bar{\mathcal{J}}_{\text{SMC}}$ (if trained with AESMC) evaluated on a test set of 100 sequences with number of particles $K = 20$.

5.4 Moving MNIST

In this experiment, we consider the *Moving MNIST* dataset introduced by [Srivastava et al. \[2015\]](#). This dataset consist of test sequences $y_{1:T}^{(n)}$ where $y_t^{(n)} \in [0, 1]^{4096}$ is a flattened matrix of greyscale values in $[0, 1]^{64 \times 64}$ with $T = 20$. The training sequences can be generated on the fly in the following manner. Sample two MNIST digits, each being in $[0, 1]^{28 \times 28}$, from the MNIST training dataset [\[LeCun, 1998\]](#). Sample two positions uniformly at random on the 64×64 frame. Sample two velocities by sampling an angle uniformly from $[0, 2\pi)$ and assigning a fixed length. For $t = 2, \dots, T$ ($T = 20$), move each MNIST digit in the direction of its velocity, bouncing off the walls and draw each MNIST digit at its position. The test sequences are generated using the same procedure, except the MNIST digits are sampled from the MNIST test dataset.

For a fixed generative network architecture for $f_{t,\theta}$ and $g_{t,\theta}$ and proposal network architecture $q_{t,\phi}$, we compare test performance of IWAE and AESMC by optimizing $\bar{\mathcal{J}}_{\text{IS}}$ and $\bar{\mathcal{J}}_{\text{SMC}}$ respectively.

We use an LSTM-based transition $f_{t,\theta}$ with number of hidden dimensions 256. The emission $g_{t,\theta}$ is based on a “deconvolution” architecture which outputs independent pseudo-Bernoulli probabilities in

$[0, 1]^{4096}$ with the following density:

$$g_{t,\theta}(y_t|x_{1:t}) = \prod_{i=1}^{4096} (p_{t,i}^{y_{t,i}} \cdot (1 - p_{t,i})^{1-y_{t,i}}), \quad (26)$$

where $(p_{t,i})_{i=1}^{4096}$ is the output of the “deconvolution” network at time t . The proposal network $q_{t,\phi}$ is based on a left-to-right LSTM with both the input and output dimensions being 256. The number of dimensions of the latent variable is 256.

We train either using \mathcal{J}_{IS} or \mathcal{J}_{SMC} with number of particles in $\{5, 10, 20\}$ and report the corresponding objective evaluated on 100 test sequences with $K = 20$ particles. We used ADAM with the learning rate 1×10^{-3} . The right plot in Figure 4 demonstrates that AESMC converges faster than IWAE.

5.5 Moving Agents

In this experiment, we introduce a dataset called *Moving Agents*. It is based on the *Moving Balls* dataset introduced by Ondruška and Posner [2016]. *Moving Balls* consists of balls moving in a straight line on a square plane, from one edge to another. The difficulty in tracking lies in the observation model of the balls. These balls are observed through a LIDAR-like view in which objects block the visibility of everything behind them as seen from a fixed point of view. This leads to occasional occlusion of balls by other balls as they move behind each other. However, once a ball is seen for two frames, its full trajectory is deterministic.

The *Moving Agents* dataset extends the *Moving Balls* dataset to add more stochasticity that is inherent in the world. In particular, we modify the true generating transition f_{t,θ^*} to be as follows. First, each ball has a goal position on the edge of the square which itself according to a probability distribution. Second, each ball is trying to avoid the other balls. Each ball’s direction of movement is simulated by adding up repulsive forces from other balls and an attractive force to the goal, mimicking electrostatic interactions. We call these balls agents because this is a model of humans interacting in a crowd.

We empirically demonstrate AESMC first in a fully observable scenario where we have an non-occluded top-down view of the agents. Then, we consider a case where we have both occlusions and stochastic agent policies. We demonstrate that after we learn the model and amortize the proposal distributions, we can perform both reconstruction and prediction. The main challenge in prediction is to incorporate the inherent uncertainty. In a typical neural network approach to prediction, one would get a blurred output of possible futures. In AESMC, we represent the uncertainty using a weighted set of possible futures, each of which represents a distinct path, thus providing meaningful means for further decisions.

5.5.1 Fully Observable View

The first dataset consists of greyscale videos of three moving agents represented as black balls on a white background. The agents are fully observable but the transition is stochastic. The starting positions are drawn randomly along the border of the frame. The goal for each agent is the point reflection of its starting position with respect to the center. The agents move with constant velocity with the direction determined by mutual repulsive force mimicking electrostatic interactions, as well as an attractive, distance independent force towards their goal. At each time step, randomness is introduced in the form of a small probability for each agent to exchange its starting and goal position, thereby reverting its movement direction. Furthermore, each agent has a randomly drawn delay before it starts moving in the beginning.

We used 2400 sequences of 50 frames with a resolution of 32×32 for training and 600 for testing. The results can be seen in Figure 5. They show that AESMC learns faster than IWAE. Resampling allows the particles and thereby also the gradients to focus earlier on relevant trajectories. Notice that the IWAE objective first quickly rises, then briefly plateaus and then approaches the AESMC loss in the long run. Both algorithms have the same model expressivity and are trained on the same target (even if it is computed differently). Consequently, they are both capable of achieving the same long term loss.

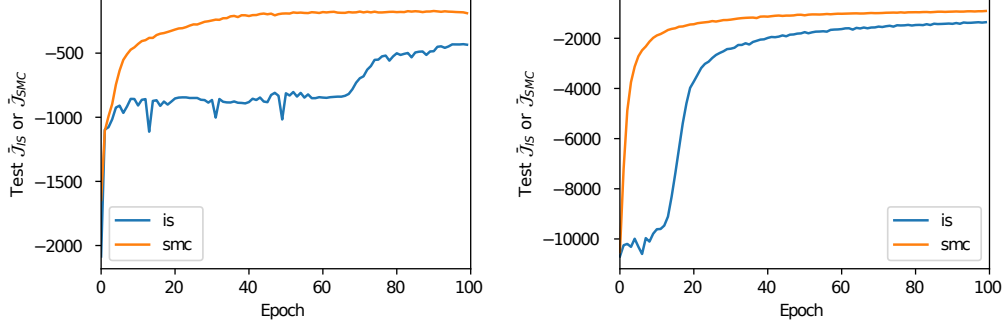


Figure 5: Simultaneous model learning and proposal amortization using IWAE and AESMC on the *Moving Agents* dataset using $K = 10$ particles. In the legend, “is” corresponds to training with IWAE and “smc” to training with AESMC. The vertical axis shows the value of either \hat{J}_{IS} (if trained with IWAE) or \hat{J}_{SMC} (if trained with AESMC). (left) Fully observable view. (right) Partially observable view.

Reconstruction For reconstruction, we use the learned values of (θ, ϕ) in order to approximate

$$p_{\theta}(\hat{y}_{1:T}|y_{1:T}) := \int p_{\theta}(\hat{y}_{1:T}|x_{1:T})p_{\theta}(x_{1:T}|y_{1:T})dx_{1:T} \quad (27)$$

using a weighted set of particles $(w_T^k, \tilde{x}_{1:T}^k)_{k=1}^K$ by sampling:

$$\hat{y}_{1:T}^k \sim p_{\theta}(y_{1:T}|\tilde{x}_{1:T}^k), \quad k = 1, \dots, K, \quad (28)$$

where the distribution in (28) is the joint emission. Thus we obtain a weighted set of particles $(w_T^k, \hat{y}_{1:T}^k)_{k=1}^K$ that characterizes $p_{\theta}(\hat{y}_{1:T}|y_{1:T})$ which can be used for approximating the maximum a-posteriori (MAP) estimator.

Prediction Similarly, we use the learned values of (θ, ϕ) in order to approximate

$$p_{\theta}(\hat{y}_{T+1:T+L}|y_{1:T}) := \int p_{\theta}(\hat{y}_{T+1:T+L}|x_{T+1:T+L})p_{\theta}(x_{T+1:T+L}|x_{1:T})p_{\theta}(x_{1:T}|y_{1:T})dx_{1:T+L} \quad (29)$$

using a weighted set of particles $(w_T^k, \tilde{x}_{1:T}^k)_{k=1}^K$ by sampling:

$$\hat{x}_{T+1:T+L}^k \sim p_{\theta}(x_{T+1:T+L}|\tilde{x}_{1:T}^k), \quad k = 1, \dots, K, \quad (30)$$

$$\hat{y}_{T+1:T+L}^k \sim p_{\theta}(\hat{y}_{T+1:T+L}|\hat{x}_{T+1:T+L}^k), \quad k = 1, \dots, K, \quad (31)$$

where the distribution in (30) is the joint transition and the one in (31) is the joint emission. Thus we obtain a weighted set of particles $(w_T^k, \hat{y}_{T+1:T+L}^k)_{k=1}^K$ that characterizes $p_{\theta}(\hat{y}_{T+1:T+L}|y_{1:T})$ which can be used for approximating the MAP estimator.

For both reconstruction and prediction, we use the inference algorithm corresponding to the one used for training to obtain the weighted characterizations of the reconstruction and prediction distributions. Both algorithms ultimately achieve very good reconstruction as well as decent prediction capabilities as can be seen in Figure 6. The first eight frames from the left show MAP reconstructions, the remaining frames show MAP predictions.

5.5.2 Partially observable state

We now turn to the occluded case. Here, the data consists of greyscale videos of visualized LIDAR observations of one moving agent and one stationary agent in front of the camera (see Figure 7). The stationary agent is preventing visibility of a large part of the area so inference is required to learn the model. The camera position is at the center of the lower border.

Agents always start on the borders on the side and move horizontally. This time there are no interactions with other agents. The goal position starts horizontally across from the starting position

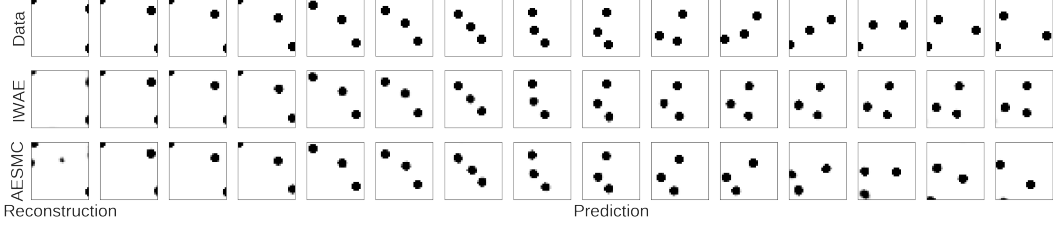


Figure 6: Ground truth data (*top*) and reconstruction and prediction as computed by IWAE (*middle*) and AESMC (*bottom*). Every third frame of the video sequence is shown. The first eight frames in the second and third row show the particle based approximation of $\text{argmax}_{\hat{y}_{1:T}} p_{\theta}(\hat{y}_{1:T}|y_{1:T})$. The next seven frames in the second and third row show the particle based approximation of $\text{argmax}_{\hat{y}_{T+1:T+L}} p_{\theta}(\hat{y}_{T+1:T+L}|y_{1:T})$. We can see that both models learn near perfect reconstructions. Exact prediction is difficult due to the randomness of involved.

and moves according to a Gaussian random walk along the border. At each time step, the agent moves to a new location drawn from a Gaussian distribution centered around a deterministically computed mean which moves it towards its current goal.

We used 4000 sequences with each 40 frames for training and 1000 for testing. Each has a resolution of 32×32 . The input data contains both the LIDAR observations (black pixels in Figure 7) as well as an image channel indicating whether a pixel is occluded (grey area in Figure 7). The results are shown on the right of in Figure 5. We find that AESMC converges faster than IS.

In Figure 7 we show the reconstruction and prediction for an example case. This time only the first four frames correspond to reconstructions with the remaining frames showing predictions. For both IWAE and AESMC we show the five particles (out of ten) which are carrying the highest weight.

The results for AESMC are exactly what we would expect: Since we start predicting the sequence while the agent is occluded, there is uncertainty in the position and time of re-appearance. Consequently, we want different particles to represent different possibilities, such that together they approximate the posterior distribution over possible paths taken by the agent. Notice that each particle represents exactly one possible path.

6 Related Work

6.1 Model Learning

Model learning in the form of maximum marginal likelihood (MML) estimation is a well-established idea, corresponding to many well-known algorithms such as expectation maximization [Dempster et al., 1977]. However, apart from the small number of cases for which the expectation can be calculated analytically, MML estimation constitutes a significantly challenging problem since it requires optimization of a target which itself corresponds to an intractable integral. It is particularly challenging to design algorithms capable of working on a wide range of models, such as the class of models corresponding to non-Markovian state space models.

Pseudo-marginal Monte Carlo [Andrieu and Roberts, 2009] and particle MCMC [Andrieu et al., 2010] methods can be used to perform Bayesian inference of both the parameters θ and latent variables x of a model. Estimation of θ can also be done as part of the SMC scheme itself by placing a prior³ $p(\theta)$ on the terms and targeting the joint $p(x, y|\theta)p(\theta)$. However, in many problems, particularly when θ is high dimensional, inferring both the parameters and the latent variables is prohibitively expensive. In many scenarios it is also necessary to have a single estimate for the parameters, for example when they have physical meaning or when prediction using the full posterior is infeasible.

As such methods rely on estimates of the marginal likelihood, rather than exact evaluations, they are in general not amenable for conventional annealing tricks (see e.g. Neal [2001]) to convert the inference problem into an optimization one by raising the likelihood to an increasingly large power. However, Doucet et al. [2002] demonstrated that *state-augmentation* can be used to anneal the target

³Note that if this prior is uniform, this preserves the target required for MML estimation.

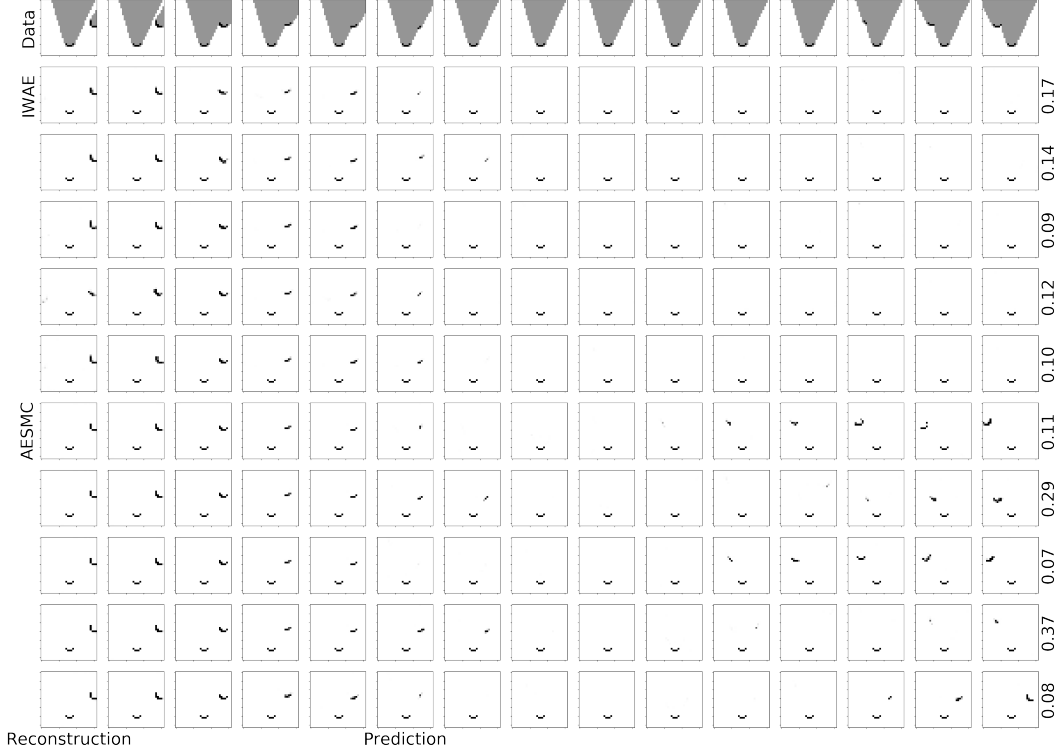


Figure 7: *Top row*: Input data, LIDAR observations in black, occluded area in grey. *Rows 2-11*: Reconstruction of the LIDAR observations in the first five frames, then prediction without taking further observations into account. *Rows 2-6* are computed using IWAE, *rows 7-11* using AESMC. $K = 10$. Reconstructions are characterized by a weighted particles set $(w_T^k, \hat{y}_{1:T}^k)_{k=1}^K$ but only top 5 weights and the corresponding $\hat{y}_{1:T}^k$ are shown. Predictions are characterized by a weighted particles set $(w_{T+1:T+L}^k, \hat{y}_{T+1:T+L}^k)_{k=1}^K$ but only top 5 weights and the corresponding $\hat{y}_{T+1:T+L}^k$ are shown. Each row corresponds to one particle out of ten used for inference. The numbers on the right denote the normalized particle weight. Particles in AESMC correctly predict different possible alternative agent paths and together approximate the posterior distribution. The actual re-appearance of the agent is stochastic and not known to the algorithm and only shown for comparison.

marginal distribution indirectly and derive a convergent MCMC based method for MML estimation. Unfortunately, this requires the target to be duplicated multiple times, leading to significant increase in the computational cost, while the use of a derivative-free proposal at each iteration can lead to slow convergence compared to gradient based schemes.

To alleviate these issues, [Doucet and Tadić \[2003\]](#) considered combining SMC with stochastic gradient methods for parameter learning. To do this they use particle methods to compute both the marginal likelihood and its gradient. This idea was later refined and extended by [Poyiadjis et al. \[2011\]](#) who also computed a particle approximation of the second derivative to apply the Newton-Raphson method for faster convergence. However, the calculation of the gradient in these methods adds additional approximation noise and higher computational cost to each SMC sweep to calculate the gradients.

[Poyiadjis et al. \[2006\]](#) considered using finite difference methods to estimate the gradients at a lower computational cost. They calculate log marginal likelihoods from independent SMC runs with permuted model parameters, from which the gradients can be estimated using the standard Kiefer-Wolfowitz FDSA technique [\[Kiefer et al., 1952\]](#). They further consider fixing the latent randomness in the process (e.g. by fixing the random number seed), but as changes to the parameters changes the weights and consequently the particle ancestry, the variance of these estimates tends to be large. Furthermore, each evaluation of the gradient requires $2D$ SMC evaluations, where D is the dimensionality of θ , substantially increasing the cost of the algorithm, particularly when D is large. [Poyiadjis et al. \[2006\]](#) considered using simultaneous perturbation stochastic approximation [\[Spall,](#)

1992] which reduces this cost to 2 SMC runs, at the expense of increased variance in the gradient estimates. In related work [Coquelin et al. \[2009\]](#), also use finite difference methods to estimate gradients for SMC, focusing on the particular application of calculating policy gradients in partially observable Markov decision processes.

[Kantas et al. \[2009\]](#) provides an overview of many of the aforementioned Monte Carlo and gradient-based methods for model-parameter estimation in SMC frameworks, along with a number of other alternatives. In particular [[Kantas et al., 2009](#), Table 1] considers and compares a number of prominent approaches to the problem of MML estimation.

More recently, [Rainforth et al. \[2016a\]](#) considered the use of Bayesian optimization alongside SMC to learn model parameters without the need for calculating gradients or annealing the target. Although they are able to overcome problems of multi-modality and provide impressive empirical results for low-dimensional problems, the use of Bayesian optimization scales poorly in both the dimensionality of the parameter space, for which the gains over random sampling diminish, and in the number of optimization iterations, for which the overhead of the Bayesian optimization calculations can become prohibitively slow.

AESMC alleviates many of the issues of these previous approaches. The use of AD means that multiple runs of SMC are no longer required to calculate each gradient, resulting in a significantly faster algorithm. The calculated gradients are also exact, given a set of evaluated particles. As we desire the gradient averaged over the latent states, these gradients are still unbiased estimates of the truth, but we show empirically that their variance is significantly lower than those of previous approaches.

6.2 Amortized Inference and Variational Autoencoders

One can see this work as extending various camps of previous related works. First, it can be seen as extending VAEs [[Kingma and Welling, 2014](#), [Rezende et al., 2014](#), [Burda et al., 2016](#)]. By posing inference amortization as adapting SMC proposal distributions, we extend the IWAES [[Burda et al., 2016](#)] which extended VAEs using IS. This allows us to consider more complicated models (e.g. time series) for which SMC is more suitable than IS. Moreover, as a result of using SMC for inference, our method performs asymptotically correct inference [[Huggins and Roy, 2015](#)], obviating the need for designing expressive variational approximations [[Mnih and Gregor, 2014](#), [Rezende and Mohamed, 2015](#), [Kingma et al., 2016](#)]. Second, it can be seen as extending previous approaches to inference amortization [[Stuhlmüller et al., 2013](#), [Paige and Wood, 2016](#), [Le et al., 2017](#)] by including the crucial element of model learning. Finally, we can see this as a unification of these concepts, in particular VAEs and inference amortization using SMC.

7 Conclusions

We have introduced, AESMC, a method performing model learning and inference amortization for SMC models. Our approach is based on considering the marginal likelihood estimator of SMC to be a deterministic function of all the variables generated during a sweep, such that its derivative can be calculated using an automatic differentiation scheme. As the expectation over all these variables is the true marginal likelihood, we can use this gradient as an input to a SGA scheme to learn both model and proposal parameters. We further show that this process can be amortized over multiple datasets, learning as system that at run time takes in a dataset and provides the optimal model and proposal for that dataset. Our approach utilizes the efficiency of SMC in performing inference and on the flexibility of deep neural networks to model complex conditional probability distributions. We have first shown the utility of our approach in the context of learning global parameters of a given SMC model framework, where we demonstrate that our approach provides lower variance gradient estimates the previous approaches. We have second shown that our approach outperforms existing approaches for simultaneous model learning and inference amortization, including existing auto-encoder approaches based on importance sampling.

References

- C. Andrieu and G. O. Roberts. The pseudo-marginal approach for efficient Monte Carlo computations. *The Annals of Statistics*, pages 697–725, 2009.
- C. Andrieu, A. Doucet, and R. Holenstein. Particle Markov chain Monte Carlo methods. *Journal of the Royal Statistical Society: Series B (Statistical Methodology)*, 72(3):269–342, 2010.
- J. Bérard, P. Del Moral, A. Doucet, et al. A lognormal central limit theorem for particle approximations of normalizing constants. *Electronic Journal of Probability*, 19(94):1–28, 2014.
- N. Boulanger-Lewandowski, Y. Bengio, and P. Vincent. Modeling temporal dependencies in high-dimensional sequences: Application to polyphonic music generation and transcription. In J. Langford and J. Pineau, editors, *Proceedings of the 29th International Conference on Machine Learning (ICML-12)*, ICML ’12, pages 1159–1166, New York, NY, USA, July 2012. Omnipress. ISBN 978-1-4503-1285-1.
- Y. Burda, R. Grosse, and R. Salakhutdinov. Importance weighted autoencoders. In *ICLR*, 2016.
- J. Chung, C. Gülçehre, K. Cho, and Y. Bengio. Gated feedback recurrent neural networks. In *ICML*, pages 2067–2075, 2015.
- P.-A. Coquelin, R. Deguest, and R. Munos. Particle filter-based policy gradient in pomdps. In *NIPS*, pages 337–344, 2009.
- P. Del Moral. Feynman-Kac formulae: genealogical and interacting particle systems with applications. *Probability and its applications*, 2004.
- A. P. Dempster, N. M. Laird, and D. B. Rubin. Maximum likelihood from incomplete data via the em algorithm. *Journal of the royal statistical society. Series B (methodological)*, pages 1–38, 1977.
- R. Douc and O. Cappé. Comparison of resampling schemes for particle filtering. In *ISPA*, pages 64–69. IEEE, 2005.
- A. Doucet and A. M. Johansen. A tutorial on particle filtering and smoothing: Fifteen years later. *Handbook of nonlinear filtering*, 12(656-704):3, 2009.
- A. Doucet and V. B. Tadić. Parameter estimation in general state-space models using particle methods. *Annals of the institute of Statistical Mathematics*, 55(2):409–422, 2003.
- A. Doucet, S. J. Godsill, and C. P. Robert. Marginal maximum a posteriori estimation using Markov chain Monte Carlo. *Statistics and Computing*, 12(1):77–84, 2002.
- S. Gershman and N. D. Goodman. Amortized inference in probabilistic reasoning. In *Proceedings of the Thirty-Sixth Annual Conference of the Cognitive Science Society*, 2014.
- Z. Ghahramani. Probabilistic machine learning and artificial intelligence. *Nature*, 521(7553):452–459, 2015.
- S. Gu, Z. Ghahramani, and R. E. Turner. Neural adaptive sequential Monte Carlo. In *NIPS*, pages 2629–2637, 2015.
- S. Hochreiter and J. Schmidhuber. Long short-term memory. *Neural computation*, 9(8):1735–1780, 1997.
- J. H. Huggins and D. M. Roy. Convergence of sequential Monte Carlo-based sampling methods. *arXiv preprint arXiv:1503.00966*, 2015.
- T. Jin, T. A. Le, M. Igl, T. Rainforth, and F. Wood. Differentiating through sequential monte carlo for model learning. Manuscript submitted for publication, March 2017.
- N. Kantas, A. Doucet, S. S. Singh, and J. M. Maciejowski. An overview of sequential Monte Carlo methods for parameter estimation in general state-space models. *IFAC Proceedings Volumes*, 42(10):774–785, 2009.
- J. Kiefer, J. Wolfowitz, et al. Stochastic estimation of the maximum of a regression function. *The Annals of Mathematical Statistics*, 23(3):462–466, 1952.
- D. Kingma and J. Ba. Adam: A method for stochastic optimization. *arXiv preprint arXiv:1412.6980*, 2014.
- D. P. Kingma and M. Welling. Auto-encoding variational Bayes. In *ICLR*, 2014.
- D. P. Kingma, T. Salimans, and M. Welling. Improving variational inference with inverse autoregressive flow. *arXiv preprint arXiv:1606.04934*, 2016.

- R. G. Krishnan, U. Shalit, and D. Sontag. Structured inference networks for nonlinear state space models. In *AAAI*, 2017.
- T. A. Le, A. G. Baydin, and F. Wood. Inference Compilation and Universal Probabilistic Programming. In *Proceedings of the 20th International Conference on Artificial Intelligence and Statistics*, pages 1338–1348, 2017.
- Y. LeCun. The mnist database of handwritten digits. 1998. URL <http://yann.lecun.com/exdb/mnist/>.
- A. Mnih and K. Gregor. Neural variational inference and learning in belief networks. In *Proceedings of The 31st International Conference on Machine Learning*, pages 1791–1799, 2014.
- C. A. Naesseth, F. Lindsten, and T. B. Schön. Sequential Monte Carlo for graphical models. In *NIPS*, pages 1862–1870, 2014.
- R. M. Neal. Annealed importance sampling. *Statistics and computing*, 11(2):125–139, 2001.
- P. Ondruška and I. Posner. Deep tracking: Seeing beyond seeing using recurrent neural networks. In *AAAI Conference on Artificial Intelligence*, 2016.
- B. Paige and F. Wood. Inference networks for sequential Monte Carlo in graphical models. In *ICML*, volume 48, 2016.
- G. Poyiadjis, S. S. Singh, and A. Doucet. Gradient-free maximum likelihood parameter estimation with particle filters. In *American Control Conference, 2006*, pages 6–pp. IEEE, 2006.
- G. Poyiadjis, A. Doucet, S. S. Singh, et al. Particle approximations of the score and observed information matrix in state space models with application to parameter estimation. *Biometrika*, 98(1):65–80, 2011.
- T. Rainforth, T.-A. Le, J.-W. van de Meent, M. A. Osborne, and F. Wood. Bayesian optimization for probabilistic programs. In *NIPS*, pages 280–288, 2016a.
- T. Rainforth, C. A. Naesseth, F. Lindsten, B. Paige, J.-W. van de Meent, A. Doucet, and F. Wood. Interacting particle Markov chain Monte Carlo. In *ICML*, volume 48, 2016b.
- D. Rezende and S. Mohamed. Variational inference with normalizing flows. In *ICML*, pages 1530–1538, 2015.
- D. J. Rezende, S. Mohamed, and D. Wierstra. Stochastic backpropagation and approximate inference in deep generative models. In *ICML*, 2014.
- H. Robbins and S. Monro. A stochastic approximation method. *The annals of mathematical statistics*, pages 400–407, 1951.
- S. Roweis and Z. Ghahramani. A unifying review of linear gaussian models. *Neural computation*, 11(2):305–345, 1999.
- J. Schulman, N. Heess, T. Weber, and P. Abbeel. Gradient estimation using stochastic computation graphs. In *NIPS*, pages 3528–3536, 2015.
- J. C. Spall. Multivariate stochastic approximation using a simultaneous perturbation gradient approximation. *IEEE transactions on automatic control*, 37(3):332–341, 1992.
- N. Srivastava, E. Mansimov, and R. Salakhutdinov. Unsupervised learning of video representations using lstms. In *ICML*, pages 843–852, 2015.
- A. Stuhlmüller, J. Taylor, and N. Goodman. Learning stochastic inverses. In *Advances in neural information processing systems*, pages 3048–3056, 2013.
- R. J. Williams. Simple statistical gradient-following algorithms for connectionist reinforcement learning. *Machine learning*, 8(3-4):229–256, 1992.
- F. Wood, J. W. van de Meent, and V. Mansinghka. A new approach to probabilistic programming inference. In *Proceedings of the Seventeenth International Conference on Artificial Intelligence and Statistics*, pages 1024–1032, 2014.

A Optimizing Objective Learns Model and Amortizes Proposals

In VAEs, given a dataset $(y^{(n)})_{n=1}^N$, we maximize the empirical average of ELBOs:

$$\operatorname{argmax}_{\theta, \phi} \frac{1}{N} \sum_{n=1}^N \text{ELBO}(\theta, \phi, y^{(n)}) \quad (32)$$

where

$$\text{ELBO}(\theta, \phi, y) = \int q_{\phi}(x|y) [\log p_{\theta}(x, y) - \log q_{\phi}(x|y)] dx. \quad (33)$$

It can be shown that

$$\text{ELBO}(\theta, \phi, y) + \text{KL}(q_{\phi}(x|y) || p_{\theta}(x|y)) = \log p_{\theta}(y) \quad (34)$$

and so we can say “by maximizing the empirical average of ELBOs, we learn the model and amortize inference”.

A.1 Variational Auto-Encoders

We will show that (34) holds, but using a different notation that will be more amenable for showing these things for the IS and SMC cases.

Let the probability densities

- $P(x) := p_{\theta}(x|y)$,
- $Z_P P(x) := p_{\theta}(x, y)$ and hence, $Z_P = p_{\theta}(y)$,
- $Q(x) := q_{\phi}(x|y)$.

Dropping the dependence on θ, ϕ , let

$$\text{ELBO} := \int Q(x) \log \frac{Z_P P(x)}{Q(x)} dx. \quad (35)$$

To show (34),

$$\text{ELBO} + \text{KL}(Q || P) = \int Q(x) \log \frac{Z_P P(x)}{Q(x)} dx + \int Q(x) \log \frac{Q(x)}{P(x)} dx \quad (36)$$

$$= \int Q(x) [\log Z_P + \log P(x) - \log Q(x) + \log Q(x) - \log P(x)] dx \quad (37)$$

$$= \int Q(x) \log Z_P dx \quad (38)$$

$$= \log Z_P. \quad (39)$$

We will re-use this identity with different underlying support of x and y in the next sections.

A.2 Importance Weighted Auto-Encoders

Here, the ELBO is

$$\text{ELBO}_{\text{IS}} := \int \left(\prod_{k=1}^K q_{\phi}(x^k|y) \right) \log \hat{Z}_{\text{IS}} dx^{1:K}, \quad (40)$$

where \hat{Z}_{IS} is the IS evidence estimator:

$$\hat{Z}_{\text{IS}} := \frac{1}{K} \sum_{k=1}^K \frac{p_{\theta}(x^k, y)}{q_{\phi}(x^k|y)}. \quad (41)$$

Let

- $Q(x^{1:K}) := \prod_{k=1}^K q_\phi(x^k|y)$,
- $\frac{Z_P P(x^{1:K})}{Q(x^{1:K})} := \hat{Z}_{\text{IS}}$, hence

$$Z_P P(x^{1:K}) = \hat{Z}_{\text{IS}} Q(x^{1:K}), \quad (42)$$

$$\text{ELBO}_{\text{IS}} = \int Q(x^{1:K}) \log \frac{Z_P P(x^{1:K})}{Q(x^{1:K})} dx^{1:K}. \quad (43)$$

First,

$$\text{ELBO}_{\text{IS}} + \text{KL}(Q||P) = \log Z_P. \quad (44)$$

Second, let's show that $Z_P = p_\theta(y)$. To show this, integrate both sides of (42):

$$Z_P = \int \hat{Z}_{\text{IS}} Q(x^{1:K}) dx^{1:K} \quad (45)$$

$$= p_\theta(y) \quad (46)$$

where the second equality arises from the unbiasedness of the IS evidence estimator.

Third, note that

$$P(x^{1:K}) = \hat{Z}_{\text{IS}} Q(x^{1:K}) / Z_P \quad (47)$$

$$= \frac{1}{K} \sum_{k=1}^K \frac{p_\theta(x^k, y)}{q_\phi(x^k|y)} Q(x^{1:K}) / p_\theta(y) \quad (48)$$

$$= \frac{1}{K} \sum_{k=1}^K \frac{Q(x^{1:K})}{q_\phi(x^k|y)} p_\theta(x^k|y) \quad (49)$$

Fourth, substituting in the original quantities,

$$\text{KL}(Q||P) = \text{KL} \left(\prod_{k=1}^K q_\phi(x^k|y) \left\| \frac{1}{K} \sum_{k=1}^K \frac{Q(x^{1:K})}{q_\phi(x^k|y)} p_\theta(x^k|y) \right\| \right). \quad (50)$$

This KL divergence is zero if and only if $q_\phi(x|y) = p_\theta(x|y)$.

Hence, we can say that “maximizing ELBO_{IS} simultaneously learns the model and amortizes IS proposals” where

- “learns the model” means maximize $\log p_\theta(y)$ and
- “amortizes IS proposals means” means make $q_\phi(x|y) = p_\theta(x|y)$.

A.3 Auto-Encoding Sequential Monte Carlo

In this section we more formally consider the derived ELBO for SMC and demonstrate a number of results. For now we will drop the dependence on θ, ϕ to unclutter the notation. It will be unnecessary for this more formal consideration to use the generic sequence-of-targets version of SMC. Specifically let

$$\pi_t(x_{1:t}) := \frac{\gamma_t(x_{1:t})}{Z_t} \quad (51)$$

be the series of normalized targets densities approximated by our SMC scheme where $\gamma_t(x_{1:t})$ and $Z_t := \int \pi_t(x_{1:t}) dx_{1:t}$ are the corresponding unnormalized targets and normalization constants respectively. The overall normalization constant for the SMC is given by $Z := Z_T$. Let $q_1(x_1)$ denote the first proposal density and $q_t(x_t|x_{1:t-1})$ the intermediate proposal densities. The particle weights (assuming resampling is carried out at each step t) are now given by

$$w_1^k = \frac{\gamma_1(x_1^k)}{q_1(x_1^k)} \quad (52)$$

$$w_t^k = \frac{\gamma_t(\tilde{x}_{1:t}^k)}{\gamma_{t-1}(\tilde{x}_{1:t-1}^{a_{t-1}^k}) q_t(x_t^k|\tilde{x}_{1:t-1}^{a_{t-1}^k})} \quad (53)$$

Running SMC and then sampling one of the produced particles in proportion to its relative weight induces the following distribution over all the generated variables

$$Q_{\text{SMC}}(x_{1:T}^{1:K}, a_{1:T-1}^{1:K}, c) := \left(\frac{w_T^c}{\sum_{\ell=1}^K w_T^\ell} \right) \left(\prod_{k=1}^K q_1(x_1^k) \right) \left(\prod_{t=2}^T \prod_{k=1}^K q_t(x_t^k | \tilde{x}_{1:t-1}^{a_{1:t-1}^k}) \right) \left(\prod_{t=1}^{T-1} \prod_{k=1}^K \frac{w_t^{a_t^k}}{\sum_{\ell=1}^K w_t^\ell} \right). \quad (54)$$

where c is index of the chosen particle. As shown by [Del Moral \[2004\]](#)

$$\hat{Z}_{\text{SMC}}(x_{1:T}^{1:K}, a_{1:T-1}^{1:K}) := \prod_{t=1}^T \frac{1}{K} \sum_{k=1}^K w_t^k \quad (55)$$

is now an unbiased estimator of Z , in the sense that

$$\mathbb{E}_{Q_{\text{SMC}}(x_{1:T}^{1:K}, a_{1:T-1}^{1:K}, c)} [\hat{Z}_{\text{SMC}}(x_{1:T}^{1:K}, a_{1:T-1}^{1:K})] = Z. \quad (56)$$

We now define the ELBO for SMC as⁴

$$\text{ELBO}_{\text{SMC}} := \int Q_{\text{SMC}}(x_{1:T}^{1:K}, a_{1:T-1}^{1:K}, c) \log \hat{Z}_{\text{SMC}}(x_{1:T}^{1:K}, a_{1:T-1}^{1:K}) dx_{1:T}^{1:K} da_{1:T-1}^{1:K} dc \quad (57)$$

and define the extended target

$$P(x_{1:T}^{1:K}, a_{1:T-1}^{1:K}, c) := \frac{Q_{\text{SMC}}(x_{1:T}^{1:K}, a_{1:T-1}^{1:K}, c) \hat{Z}_{\text{SMC}}(x_{1:T}^{1:K}, a_{1:T-1}^{1:K})}{Z} \quad (58)$$

in a similar manner as done in [Andrieu et al. \[2010\]](#) and [Rainforth et al. \[2016b\]](#). Now by (56), we have that

$$\int P(x_{1:T}^{1:K}, a_{1:T-1}^{1:K}, c) dx_{1:T}^{1:K} da_{1:T-1}^{1:K} dc = 1$$

and thus that $P(x_{1:T}^{1:K}, a_{1:T-1}^{1:K}, c)$ is a normalized probability density. Furthermore, by (41) of [Andrieu et al. \[2010\]](#) then $P(x_{1:T}^{1:K}, a_{1:T-1}^{1:K}, c)$ is the extended distribution targeted by the PIMH algorithm and [Andrieu et al. \[2010\]](#) show that the marginal of this distribution is the target, namely

$$\int P(x_{1:T}^{1:K}, a_{1:T-1}^{1:K}, c) dx_{1:T}^{1:K \setminus c} da_{1:T-1}^{1:K} dc = P(\hat{x}_{1:T}) = \pi_T(\hat{x}_{1:T}). \quad (59)$$

where $\hat{x}_{1:T}$ is the returned particle from sampling from $P(x_{1:T}^{1:K}, a_{1:T-1}^{1:K}, c)$ and then taking $\tilde{x}_{1:T}^c$ as the output.

We can now rewrite the ELBO as follows

$$\text{ELBO}_{\text{SMC}} = \int Q_{\text{SMC}}(x_{1:T}^{1:K}, a_{1:T-1}^{1:K}, c) \log \left(Z \frac{P(x_{1:T}^{1:K}, a_{1:T-1}^{1:K}, c)}{Q_{\text{SMC}}(x_{1:T}^{1:K}, a_{1:T-1}^{1:K}, c)} \right) dx_{1:T}^{1:K} da_{1:T-1}^{1:K} dc \quad (60)$$

from which it immediately follows that

$$\text{ELBO}_{\text{SMC}} + \text{KL}(Q_{\text{SMC}} \| P) = \log Z. \quad (61)$$

Now as $\text{KL}(Q_{\text{SMC}} \| P) \geq 0$ and $\text{KL}(Q_{\text{SMC}} \| P) = 0$ if and only if $Q_{\text{SMC}}(x_{1:T}^{1:K}, a_{1:T-1}^{1:K}, c) = P(x_{1:T}^{1:K}, a_{1:T-1}^{1:K}, c)$ for all $(x_{1:T}^{1:K}, a_{1:T-1}^{1:K}, c)$, we see that ELBO_{SMC} is maximized if and only if $Q_{\text{SMC}} = P$. Furthermore, we see from (58) that when this is true, we have $\hat{Z}_{\text{SMC}}(x_{1:T}^{1:K}, a_{1:T-1}^{1:K}) = Z$ for all $(x_{1:T}^{1:K}, a_{1:T-1}^{1:K}, c)$. In other words, if Q_{SMC} is capable of completely encapsulating P and we find the global maximum of ELBO_{SMC} , then the resulting estimator gives exact estimates for the marginal likelihood.

⁴Note that the inclusion of c means that the form of given here is slightly different to the main paper, as is the form Q_{SMC} . However, as \hat{Z}_{SMC} is independent of c , the integration over c simply removes the $\frac{w_T^c}{\sum_{\ell=1}^K w_T^\ell}$ term from (54), mean that the two definitions of ELBO_{SMC} are equivalent.

If we now rewrite (61) to explicitly include the dependencies

$$\begin{aligned} \text{ELBO}_{\text{SMC}}(\theta, \phi, y_{1:T}^{(n)}) + \text{KL} \left(Q_{\text{SMC}} \left(x_{1:T}^{1:K}, a_{1:T-1}^{1:K}, c, \phi, y_{1:T}^{(n)} \right) \middle| \middle| P \left(x_{1:T}^{1:K}, a_{1:T-1}^{1:K}, c, \theta, y_{1:T}^{(n)} \right) \right) \\ = \log Z(\theta, y_{1:T}^{(n)}) \end{aligned} \quad (62)$$

then we see that if we optimize $\text{ELBO}_{\text{SMC}}(\theta, \phi, y_{1:T}^{(n)})$ with respect to model parameters θ and proposal parameters ϕ for a given $y_{1:T}^{(n)}$ then we a) find the model that optimizes the marginal likelihood $Z(\theta, y_{1:T}^{(n)})$ and b) find the best possible proposal for that model. We can further consider amortization by optimizing $\frac{1}{N} \sum_{n=1}^N \text{ELBO}_{\text{SMC}}(\theta, \phi, y_{1:T}^{(n)})$ with respect to ϕ and θ .

A.3.1 Implications of Optimizing ELBO on Proposal and Target Decomposition

We now consider what the implications of these results are for the per sample proposals and intermediary target distributions when the ELBO_{SMC} is maximized. We first consider the implied characterization of $q_{\phi^*}(\hat{x}_{1:T})$ where ϕ^* is the optimal proposal parameters,

$$q_{\phi^*}(\hat{x}_{1:T}) = \int Q_{\text{SMC}}(x_{1:T}^{1:K}, a_{1:T-1}^{1:K}, c, \phi^*) dx_{1:T}^{1:K \setminus c} da_{1:T-1}^{1:K} dc,$$

and we omit dependency $y_{1:T}^{(n)}$ to avoid clutter. We can immediately see that as $Q_{\text{SMC}}(x_{1:T}^{1:K}, a_{1:T-1}^{1:K}, c, \phi^*) = P(x_{1:T}^{1:K}, a_{1:T-1}^{1:K}, c, \theta^*)$, then

$$q_{\phi^*}(\hat{x}_{1:T}) = \pi_{T, \theta^*}(\hat{x}_{1:T}) \quad (63)$$

using (59) and the fact having the same joint distribution implies the same marginal distributions. Thus the overall proposal distribution corresponds to the target distribution when the ELBO_{SMC} is maximized.

Next we simultaneously consider the characterization of the intermediary targets and proposals. To do this we first consider marginal proposals on $\hat{x}_{1:t}$

$$q_{t, \phi^*}(\hat{x}_{1:t}) = \int \pi_{T, \theta^*}(\hat{x}_{1:T}) d\hat{x}_{t+1:T} := \hat{\pi}_{t, \theta^*}(\hat{x}_{1:t}) \quad (64)$$

where $\hat{\pi}_{t, \theta^*}$ is a normalized marginal of π_{T, θ^*} and need not be equal to corresponding intermediary target π_{t, θ^*} . We now see that for all $k \in \{1, \dots, K\}$

$$q_{t, \phi^*}(x_t^k | \hat{x}_{1:t-1}^{a_{t-1}^k}) = \frac{q_{t, \phi^*}(\tilde{x}_{1:t}^k)}{\int q_{t, \phi^*}(\tilde{x}_{1:t}^k) dx_t^k} = \frac{\hat{\pi}_{t, \theta^*}(\tilde{x}_{1:t}^k)}{\hat{\pi}_{t-1, \theta^*}(\tilde{x}_{1:t-1}^{a_{t-1}^k})} = \frac{\check{Z}_{t-1}}{\check{Z}_t} \frac{\hat{\gamma}_{t, \theta^*}(\tilde{x}_{1:t}^k)}{\hat{\gamma}_{t-1, \theta^*}(\tilde{x}_{1:t-1}^{a_{t-1}^k})} \quad (65)$$

where $\hat{\gamma}_{t, \theta^*}(\hat{x}_{1:t})$ is the unnormalized version for $\hat{\pi}_{t, \theta^*}(\hat{x}_{1:t})$ with corresponding normalization constant \check{Z}_t with $\check{Z}_0 = 1$. The associated weights are now given as follows

$$w_t^k = \frac{\gamma_{t, \theta^*}(\tilde{x}_{1:t}^k)}{\gamma_{t-1, \theta^*}(\tilde{x}_{1:t-1}^{a_{t-1}^k}) q_{t, \phi^*}(x_t^k | \tilde{x}_{1:t-1}^{a_{t-1}^k})} = \frac{\check{Z}_t}{\check{Z}_{t-1}} \frac{\gamma_{t, \theta^*}(\tilde{x}_{1:t}^k)}{\gamma_{t-1, \theta^*}(\tilde{x}_{1:t-1}^{a_{t-1}^k})} \frac{\hat{\gamma}_{t-1, \theta^*}(\tilde{x}_{1:t-1}^{a_{t-1}^k})}{\hat{\gamma}_{t, \theta^*}(\tilde{x}_{1:t}^k)} \quad (66)$$

which gives the marginal likelihood estimate

$$\hat{Z}_{\text{SMC}} = \prod_{t=1}^T \frac{1}{K} \sum_{k=1}^K w_t^k \quad (67)$$

$$= \prod_{t=1}^T \frac{1}{K} \sum_{k=1}^K \frac{\check{Z}_t}{\check{Z}_{t-1}} \frac{\gamma_{t, \theta^*}(\tilde{x}_{1:t}^k)}{\gamma_{t-1, \theta^*}(\tilde{x}_{1:t-1}^{a_{t-1}^k})} \frac{\hat{\gamma}_{t-1, \theta^*}(\tilde{x}_{1:t-1}^{a_{t-1}^k})}{\hat{\gamma}_{t, \theta^*}(\tilde{x}_{1:t}^k)} \quad (68)$$

$$= \check{Z}_T \prod_{t=1}^T \frac{1}{K} \sum_{k=1}^K \frac{\gamma_{t, \theta^*}(\tilde{x}_{1:t}^k)}{\hat{\gamma}_{t, \theta^*}(\tilde{x}_{1:t}^k)} \frac{\hat{\gamma}_{t-1, \theta^*}(\tilde{x}_{1:t-1}^{a_{t-1}^k})}{\gamma_{t-1, \theta^*}(\tilde{x}_{1:t-1}^{a_{t-1}^k})}. \quad (69)$$

We now consider what happens if $\hat{\gamma}_{t,\theta^*} = \gamma_{t,\theta^*}$. This first implies that all of the terms in the sum of K in (69) must equal one, which gives $\hat{Z}_{\text{SMC}} = \check{Z}_T$. Furthermore, $\hat{\gamma}_{t,\theta^*} = \gamma_{t,\theta^*}$ implies that each $\check{Z}_t = Z_t$ and therefore that $\hat{Z}_{\text{SMC}} = Z_T = Z$. Thus if $\hat{\gamma}_{t,\theta^*} = \gamma_{t,\theta^*}$ the marginal likelihood estimate is a zero-variance estimate for the truth, as expected by the result that the ELBO_{SMC} is maximized if and only if $\hat{Z}_{\text{SMC}} = Z$ for all $(x_{1:T}^{1:K}, a_{1:T-1}^{1:K})$. Furthermore, $\hat{\gamma}_{t,\theta^*} = \gamma_{t,\theta^*}$ implies that $\hat{\pi}_{t,\theta^*} = \pi_{t,\theta^*}$ and therefore $q_{t,\phi^*} = \pi_{t,\theta^*}$ by (64). In other words, the ELBO_{SMC} is maximized when all the intermediary proposals are also exact samples from the corresponding marginals of the target distribution.

On the contrary, if $\hat{\pi}_{t,\theta^*} \neq \pi_{t,\theta^*}$ then it is easy to construct counter examples where $\hat{Z}_{\text{SMC}} \neq Z$ for some $(x_{1:T}^{1:K}, a_{1:T-1}^{1:K})$. Furthermore, intuitively unless all the weights are equal then one would not expect the marginal likelihood estimate to be zero variance as one can consider removing a

sample which would then change the estimate. We see that the term $\frac{\gamma_{t,\theta^*}(\tilde{x}_{1:t}^k)}{\hat{\gamma}_{t,\theta^*}(\tilde{x}_{1:t}^k)} \frac{\gamma_{t-1,\theta^*}(\tilde{x}_{1:t-1}^{a_k^{k-1}})}{\gamma_{t-1,\theta^*}(\tilde{x}_{1:t-1}^{a_k^{k-1}})}$ has to

be constant for the weights to be equal, and thus it follows that the ELBO_{SMC} is maximized only when this holds.

Here we have presumed that we can fully manipulate the series of targets for the SMC sweep. For models where the likelihood of some datapoints depends on more than the current latent state, i.e. $g_{t,\theta}(y_t|x_{1:t}) \neq g_{t,\theta}(y_t|x_t)$ this means that the learnt intermediary targets will need to depend on more than just the current corresponding data point. This is not a problem when the relationship $g_{t,\theta}(y_t|x_{1:t}) = g_{t,\theta}(y_t|x_t) \forall t \in 1:T$ holds (as is the case for the AESMC experiments considered) or whenever θ and ϕ parametrize sufficiently flexible models to specify the required arbitrary series of targets or, but it can have implications when neither of these is the case. In such a scenario, it is not possible to achieve $\text{KL}(Q_{\text{SMC}}||P) = 0$, and the so called one-step optimal proposal [Doucet and Johansen \[2009\]](#) may be best than can be achieved. We leave characterizing the implication of optimizing the ELBO in such cases, but reiterate that this can always be solved using a sufficiently flexible model family and proposal to allow appropriate adaptation of the series of targets.

B Neural Network Architectures

B.1 Transition models

B.1.1 GRU

$$f_{t,\theta}(x_t|x_{1:t-1}) = \text{Normal}(x_t|\mu_t, \sigma_t^2), \quad (70)$$

$$\mu_t = (1 - g_t) \odot \text{Linear}(x_{t-1}, \text{latentdim}, \text{latentdim}) + g_t \odot h_t, \quad (71)$$

$$\sigma_t^2 = \text{Softplus}(\text{Linear}(\text{ReLU}(h_t), \text{latentdim}, \text{latentdim})), \quad (72)$$

$$g_t = \text{Sigmoid}(\text{Linear}(\text{ReLU}(\text{Linear}(x_{t-1}, \text{latentdim}, \text{hiddendim})), \text{hiddendim}, \text{latentdim})), \quad (73)$$

$$h_t = \text{Linear}(\text{ReLU}(\text{Linear}(x_{t-1}, \text{latentdim}, \text{hiddendim})), \text{hiddendim}, \text{latentdim}). \quad (74)$$

B.1.2 LSTM

$$x_t = z_{t-1} \quad (75)$$

$$i_t = \text{Sigmoid}(\text{Linear}(x_t) + \text{Linear}(h_{t-1})) \quad (76)$$

$$f_t = \text{Sigmoid}(\text{Linear}(x_t) + \text{Linear}(h_{t-1})) \quad (77)$$

$$g_t = \text{Tanh}(\text{Linear}(x_t) + \text{Linear}(h_{t-1})) \quad (78)$$

$$o_t = \text{Sigmoid}(\text{Linear}(x_t) + \text{Linear}(h_{t-1})) \quad (79)$$

$$c_t = f_t \odot c_{t-1} + i_t \odot g_t \quad (80)$$

$$h_t = o_t \odot \text{Tanh}(c_t) \quad (81)$$

$$\mu_t = \text{Linear}(h_t) \quad (82)$$

$$\sigma_t^2 = \text{Softplus}(\text{Linear}(h_t)) \quad (83)$$

$$z_t = \mathcal{N}(\mu_t, \sigma_t^2) \quad (84)$$

B.2 Emission models

B.2.1 MLP

$$g_{t,\theta}(y_t|x_{1:t}) = \text{Bernoulli}(p_t) \quad (85)$$

$$p_t = \text{Sigmoid}(\text{Linear}(\text{ReLU}(\text{Linear}(x_t, \text{latentdim}, \text{hiddendim})), \text{hiddendim}, \text{obsdim})). \quad (86)$$

B.2.2 Deconvolution

$$o_t = \text{Deconv2d} \circ \text{LeakyReLU} \circ \text{Batchnorm} \circ \text{Deconv2d} \quad (87)$$

$$\circ \text{LeakyReLU} \circ \text{Batchnorm} \circ \text{Deconv2d} \quad (88)$$

$$\circ \text{LeakyReLU} \circ \text{Batchnorm} \circ \text{Deconv2d}(z_t) \quad (89)$$

B.3 Proposal networks

Right-to-Left

$$q_{t,\phi}(x_t|y_{t:T}, x_{1:t-1}) = \text{Normal}(x_t|\mu_{q,t}, \sigma_{q,t}^2) \quad (90)$$

$$\mu_{q,t}, \sigma_{q,t}^2 = \text{Combiner}(x_{t-1}, y_{t:T}) \quad (91)$$

Left-to-Right

$$q_{t,\phi}(x_t|y_{1:t}, x_{1:t-1}) = \text{Normal}(x_t|\mu_{q,t}, \sigma_{q,t}^2) \quad (92)$$

$$\mu_{q,t}, \sigma_{q,t}^2 = \text{Combiner}(x_{t-1}, y_{1:t}) \quad (93)$$

B.3.1 Combiner

$$emb_t = \text{Embedder}(y_t) \quad (94)$$

$$r_t = \text{LSTM}(emb_{1:t} \text{ or } emb_{t:T}) \quad (95)$$

$$c_t = \frac{\text{Tanh}(\text{Linear}(x_{t-1})) + r_t}{2} \quad (96)$$

$$\mu_t = \text{Linear}(c_t) \quad (97)$$

$$\sigma_t^2 = \text{Softplus}(\text{Linear}(c_t)) \quad (98)$$

B.3.2 Observation Embedders

MLP

$$emb_t = \text{Linear}(\text{ReLU}(\text{Linear}(y_t))) \quad (99)$$

Convolution

$$emb_t = \text{Conv2d} \circ \text{LeakyReLU} \circ \text{Batchnorm} \circ \text{Conv2d} \quad (100)$$

$$\circ \text{LeakyReLU} \circ \text{Batchnorm} \circ \text{Conv2d} \quad (101)$$

$$\circ \text{LeakyReLU} \circ \text{Batchnorm} \circ \text{Conv2d}(y_t) \quad (102)$$